On the Effect of Triadic Closure on Network Segregation

REDIET ABEBE, University of California, Berkeley, USA
NICOLE IMMORLICA, Microsoft Research, USA
JON KLEINBERG, Cornell University, USA
BRENDAN LUCIER, Microsoft Research, USA
ALI SHIRALI, University of California, Berkeley, USA

The tendency for individuals to form social ties with others who are similar to themselves, known as homophily, is one of the most robust sociological principles. Since this phenomenon can lead to patterns of interactions that segregate people along different demographic dimensions, it can also lead to inequalities in access to information, resources, and opportunities. As we consider potential interventions that might alleviate the effects of segregation, we face the challenge that homophily constitutes a pervasive and organic force that is difficult to push back against. Designing effective interventions can therefore benefit from identifying counterbalancing social processes that might be harnessed to work in opposition to segregation.

In this work, we show that triadic closure—another common phenomenon that posits that individuals with a mutual connection are more likely to be connected to one another—can be one such process. In doing so, we challenge a long-held belief that triadic closure and homophily work in tandem. By analyzing several fundamental network models using popular integration measures, we demonstrate the desegregating potential of triadic closure. We further empirically investigate this effect on real-world dynamic networks, surfacing observations that mirror our theoretical findings. We leverage these insights to discuss simple interventions that can help reduce segregation in settings that exhibit an interplay between triadic closure and homophily. We conclude with a discussion on qualitative implications for the design of interventions in settings where individuals arrive in an online fashion, and the designer can influence the initial set of connections.

CCS Concepts: • **Theory of computation** → **Network formation**; **Random network models**; **Social networks**; • **Mathematics of computing** → **Random graphs**; • **Computing methodologies** → *Network science.*

Additional Key Words and Phrases: segregation, access to information, triadic closure, homophily, random networks, dynamic networks

1 INTRODUCTION

Segregation impacts socioeconomic inequality by influencing individuals' abilities to obtain accurate and relevant information, garner social support, and improve access to opportunity [7, 10, 11, 15, 24, 27, 38, 42, 46]. A number of different social processes can impact segregation. Among these, homophily—the process by which individuals are more likely to form ties with whom they share similarities—is one of the most robust phenomena [32, 33, 35–37, 41]. A long line of theoretical and empirical work shows that homophily can create and amplify existing segregation. And because

homophily is a potent and organic force, it is challenging to push back against without harnessing existing social processes that may already be countering its negative effects.

In this work, we show that *triadic closure*—a process in which individuals are more likely to form ties to others with whom they share mutual connections—is one such phenomenon [22, 31, 39]. That is, we show that triadic closure alleviates segregation in settings where homophily is also present. Our results, which we present for a number of well-studied network formation models, challenge a long-held belief that triadic closure amplifies the effects of homophily. Such claims are frequently made, at times informally, citing concerns that homophily may lead friends-of-friends also to be similar, which would lead to further segregation under triadic closure [5, 32, 45].

Our work challenges this intuition: Triadic closure connects people with mutual ties, and we may therefore assume that these new links reinforce existing patterns. We find, however, that the long-range nature of triadic closure can, in fact, counteract this phenomenon. In settings where homophily is present, individuals who are similar are more likely to form ties. Consequently, if friends-of-friends are not already connected, it may be because they are dissimilar. Triadic closure can therefore expose people to dissimilar individuals, thereby decreasing segregation.

Mathematically, triadic closure operates on a graph-theoretic structure called a *wedge*. Wedges consist of two nodes that have a neighbor in common but are themselves not linked. Triadic closure works by closing these wedges, i.e., by creating a link between these two nodes such that all three nodes are connected to one another. We analyze the effect of triadic closure on homophily by disaggregating wedges into monochromatic and bichromatic ones. The two nodes sharing a neighbor are of the same type in the case of the former but not the latter. We observe that the effect of triadic closure depends on the relative sizes of monochromatic and bichromatic wedges. We study this effect both in an *absolute* sense—by looking at whether network integration increases when we close a random wedge—and in a *relative* sense—by comparing the effect of closing a random wedge with that of closing a random edge.

We provide general results for a number of well-studied models, including the stochastic block model (SBM) and a popular growing network formation model by Jackson and Rogers [28], and show that triadic closure can have positive absolute and relative effects on integration in settings where there is homophily. We use these insights to study interventions on the Jackson-Rogers model and find that small changes leveraging the effects of triadic closure can have an outsized effect on mitigating segregation in the long run. We then study the interaction of homophily, triadic closure, and segregation using a large citation network where we estimate the network formation model and find that empirically observed effects of triadic closure on integration closely match our theoretical results.

Our work also generalizes a number of theoretical contributions on graph and network theory. For instance, we generalize a result about network integration from Jackson and Rogers [28] to a general network with heterogeneous nodes and with arbitrary distribution over the node types. There we provide general closed-form solutions for the time dynamic of network integration. Putting the relationship between triadic closure and homophily on a theoretical footing to ask these questions from a mathematical lens is a recent undertaking; in one formalization, Asikainen et al. [5] propose a model that combines triadic closure and random link rewiring with an underlying level of *choice homophily*, in which nodes have a base preference for linking based on similarity. They show that the combination of these forces amplifies existing patterns of homophily. We examine these findings to show that this model introduces homophily even into the triadic closure process itself. We study a general variant of the Asikainen et al. [5] model and show that triadic closure mitigates segregation when all wedges are equally likely to close under triadic closure.

The remainder of the paper is organized as follows: In Section 2, we present an analysis of triadic closure in the stochastic block model, deriving mathematical results on its absolute and

relative effects on integration. We then introduce and analyze a growing graph model based on the Jackson-Rogers model, considering the effect of triadic closure on its equilibrium state integration in Section 3. We then tackle the design of interventions that act on the initial phase of making friendships to optimize network integration. In Section 4, we study a variant of the Asikainen et al. [5] model and show that in settings where triadic closure is not a priori biased in favor of monochromatic wedges, we obtain results consistent with our above findings. Finally, we study our results empirically using a large citation network and show that we can effectively model the network formation process in Section 5. We also find that the effects of triadic closure on integration closely match our theoretical findings. We close with a discussion of related works as well as the interplay of homophily, triadic closure, integration, and implications for network interventions on- and off-line settings in Sections 6 and 7.

2 TRIADIC CLOSURE IN THE STOCHASTIC BLOCK MODEL

We begin by introducing notations and terminology which we will use throughout this paper: Let G be a heterogeneous network, i.e., a network where nodes have a *type*, which may, for instance, correspond to membership in a demographic group. We assume that there are K types. We denote the type of node i with $type(i)$. We say an edge (i, j) is *monochromatic* if $type(i) = type(j)$ and *bichromatic* otherwise.

Following convention, we measure network integration using the fraction of bichromatic edges. We denote the level of network integration at time t by $f(t)$. Smaller values correspond to more-segregated networks.

A triplet of nodes (i, h, j) is called a *wedge* if there exist edges (i, h) and (h, j) but not (i, j). A wedge is said to be monochromatic if i and j are of the same type and bichromatic if they are not. As is common in many studies of triadic closure, we assume that all wedges are equally likely to close under triadic closure. This is due to the fact that triadic closure is designed to capture the phenomena where the presence of node h in the wedge (i, h, j) impacts whether or not edge (i, j) is eventually formed, regardless of the node types.

In this section, we study Stochastic Block Models (SBM). Under SBM, we assign independent probabilities to the existence of different edges, where these probabilities depend on the types of the corresponding nodes. Given nodes i and j, edge (i, j) is formed with probability $p \in [0, 1]$ if i and j are of the same type and with probability $q \in [0, 1]$ if they are not. We say there is homophily if and only if $p > q$.

We study the effect of triadic closure in this model post network formation. That is, after the network is formed, we select and close a random wedge and measure the change in network integration. As is common in other studies on the influence of triadic closure, we first study the *absolute effect* by comparing the state of network integration before and after the intervention. Our work also explores the *relative effect* of triadic closure by considering an alternative mechanism as the baseline against which we compare the effect. We propose closing a random edge as this alternative mechanism and define relative effect as the difference in integration resulting from closing a random wedge versus a random edge.

2.1 Absolute and Relative Effects of Triadic Closure

We show that triadic closure improves network integration if and only if there is homophily.

THEOREM 2.1. *For any SBM network G with $K \geq 2$ types each consisting of n_k nodes, where $k \in [K]$, for sufficiently large values of n_k, triadic closure has positive absolute effect on network integration if and only if $p > q$.*

See proof in Appendix A .

The proof first shows that closing a random wedge increases network integration if and only if the ratio of bichromatic wedges to monochromatic wedges is larger than the ratio of bichromatic edges to monochromatic edges. We then approximate the number of wedges and edges with their expected values and show that homophily is a necessary and sufficient condition to achieve the stated result. We note that this result holds for *any* number of types as well as for cases where the types may be imbalanced in size, i.e., there may be a majority-minority partition.

Triadic closure may be improving integration simply because we are adding an edge and not because of the type of edge that was added. To untangle the effect of edge addition with that of triadic closure, we turn our attention to the relative effect.

THEOREM 2.2. *Consider the baseline of adding a random edge to an SBM network G with $K \geq 2$ types each consisting of n_k nodes, where $k \in [K]$. For sufficiently large values of n_k:*

(1) *Triadic closure has a negative relative effect on network integration if $p > q$,*
(2) *Triadic closure has positive or neutral relative effect on network integration if and only if $q \geq p \geq q\, l^*$, where*

$$l^* = \frac{2(\sum_k n_k)(\sum_k n_k^2)^2 - (\sum_k n_k)^2(\sum_k n_k^3) - (\sum_k n_k^2)(\sum_k n_k^3)}{(\sum_k n_k^3)\big((\sum_k n_k)^2 - (\sum_k n_k^2)\big)} \leq 1.$$

See proof in Appendix A .

For the case of balanced groups (i.e., when the n_k are all equal), Theorem 2.2 simplifies to:

Corollary 2.3. *For any SBM network G with $K \geq 2$ balanced types each consisting of n/K nodes, for sufficiently large values of n/K, triadic closure has a neutral relative effect if $p = q$ and negative relative effect if $p > q$.*

PROOF. This follows from Theorem 2.2 if we set $n_k = \frac{n}{K}$, which results in $l^* = 1$. □

These above results show that we can obtain diverging conclusions when we consider absolute versus relative effects of triadic closure. In doing so, they highlight the need for further precision in examining the interaction between triadic closure, homophily, and related social phenomena. Namely, to isolate the effect of social phenomena such as triadic closure, we may need to set appropriate baselines against which we are comparing their effect.

We considered adding a random edge as a natural baseline in our setting but also note that a random edge is likely to be bichromatic. Another baseline we may consider is adding a homophilous random edge, i.e., rather than adding a random edge, we favor monochromatic edges using a factor $\gamma \geq 1$. Let o_m and o_b be the expected number of monochromatic and bichromatic missing edges. The expected increase in the number of bichromatic edges after adding a γ-homophilous edge is approximately $\frac{o_b}{o_b + \gamma o_m}$. Theorem 2.4 shows that, compared to adding a homophilous edge, triadic closure has a positive relative effect if the network is sufficiently heterophilous.

THEOREM 2.4. *Consider the baseline of adding a γ-homophilous random edge to an SBM network G with $K \geq 2$ types consisting of n_k nodes, where $k \in [K]$. For sufficiently large values of n_k, triadic closure has positive or neutral relative effect on network integration if and only if $q\, u(\gamma) \geq p \geq q\, l(\gamma)$, where $u(\gamma) \geq 1$ and $l(\gamma) \leq 1$.*

See proof in Appendix A .

Note that for given p and q, solving for $u(\gamma^*) = \frac{p}{q}$ if $p \geq q$ or $l(\gamma^*) = \frac{p}{q}$ if $p < q$, provides an equivalence notion for the effect of triadic closure. In this case, the effect of closing a random wedge on network integration is the same as adding a γ^*-homophilous edge to the network.
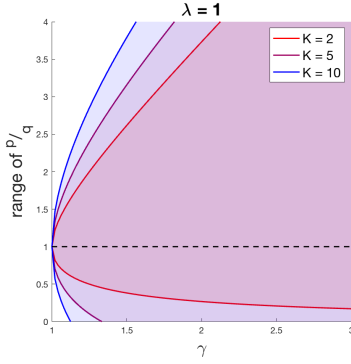
Fig. 1. $u(\gamma)$ and $l(\gamma)$ for balanced groups.
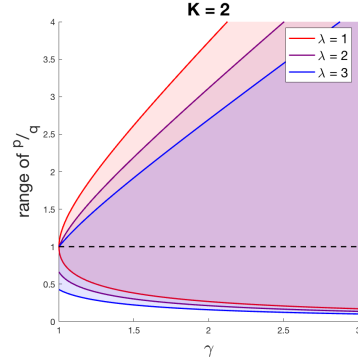
Fig. 2. $u(\gamma)$ and $l(\gamma)$ for unbalanced groups ($\lambda = 2$).

For the special case of balanced groups, Figure 1 shows $u(\gamma)$ and $l(\gamma)$ for different values of K. In this figure, the shaded area corresponds to the values of $\frac{p}{q}$ such that $u(\gamma) \geq \frac{p}{q} \geq l(\gamma)$. This is the region where triadic closure has a positive relative effect compared to adding a γ-homophilous edge. We can see that as we increase γ, triadic closure will have a more-positive effect for larger values of p. Further, we can see that $u(\gamma)$ increases for larger values of K.

To see the effect of heterogeneous sizes in the groups, we consider the case where each group k has $n_k = n_1 \lambda^k$ members. So, the larger the λ, the more variance in size across groups. Figure 2 shows $u(\gamma)$ and $l(\gamma)$ for different λ values when the number of groups is fixed. By increasing λ, we see that $u(\gamma)$ decreases, indicating that triadic closure has a less positive effect as the relative sizes between the groups increases.

2.2 Examining Other Measures of Network Health

Thus far, we have studied integration using a popular measure in the literature—the fraction of bichromatic edges. High rates of network integration can be observed in settings where we may otherwise consider the network to be brittle. We therefore consider another robust measure of network health using eigenvector centrality. By doing so, we show that the positive effect of triadic closure is not limited to the original measure of integration.

Let A be the network's adjacency matrix and $v(A)$ be the eigenvector corresponding to the largest eigenvalue of A. The eigenvector centrality of the ith node is defined as $v_i(A)$. Suppose we have a network consisting of two groups, including the setting where the groups may be imbalanced in size. Then our value of interest is the ratio of the average centrality of the minority to the average centrality of the majority group. As above, we first consider the absolute effect of triadic closure.

THEOREM 2.5. *Consider an SBM network G with two types consisting of n_1 and n_2 nodes, where $n_1 > n_2$. Let EV_k be the expected eigenvector centrality of a node from the kth group. For sufficiently large $n = n_1 + n_2$, triadic closure increases $\frac{EV_2}{EV_1}$ if and only if $p > q$.*

PROOF. Let P_{ij} be the probability that node i is connected to another node j in G. In an *SBM*, $P_{ij} = p$ if $type(i) = type(j)$ and $P_{ij} = q$ otherwise. We also set $P'_{ii} = 0$ to avoid self loops. After closing a random wedge, we call the new network G' and the new probability that i and j are connected P'_{ij}.

Let w_{ij} be the expected number of wedges in G, such that we have edges (i, h) and (h, j) exist but not (i, j). Let w be the expected total number of wedges. With mean field approximation:

$$P'_{ij} = P_{ij} + (1 - P_{ij})\frac{w_{ij}}{w}. \tag{1}$$

Here, the second term on the right hand side approximates the probability that i and j get connected after closing a random wedge. Note that $w = O(n^3)$ and $w_{ij} = O(n)$, so this term is $O\left(\frac{1}{n^2}\right)$. We find w_{ij} based on i and j's types:

$$w_{ij} = \begin{cases} (n_1 - 2)p^2 + n_2q^2 & type(i) = type(j) = 1 \\ (n_2 - 2)p^2 + n_1q^2 & type(i) = type(j) = 2 \\ (n - 2)pq & type(i) \neq type(j) \end{cases}. \tag{2}$$

By plugging w_{ij} into P'_{ij}, we note:

$$P'_{ij} = \begin{cases} p'_1 = p + (1 - p)[(n_1 - 2)p^2 + n_2q^2]\frac{1}{w} & type(i) = type(j) = 1 \\ p'_2 = p + (1 - p)[(n_2 - 2)p^2 + n_1q^2]\frac{1}{w} & type(i) = type(j) = 2 \\ q' = q + (1 - q)(n - 2)pq\frac{1}{w} & type(i) \neq type(j) \end{cases}. \tag{3}$$

Although we look for the expected eigenvector of the network, for a sufficiently large number of nodes, this quantity will be close to the eigenvector of the expected network [12, 14]. We show the expected adjacency matrix of G' by $A' = [P'_{ij}]$ and study eigenvectors of A' instead of G'.

Due to the block nature of A', it's easy to see the eigenvector corresponding to the largest eigenvalue of A', which we denote by v', has only two distinct values. Without loss of generality, we assume $v'_i = 1$ if $type(i) = 1$ and $v'_i = a = \frac{EV_2}{EV_1}$ otherwise. That is, eigenvectors have a scale ambiguity that is usually resolved by setting the norm to one. Here, we instead fix element of the vector. Since $A'v' = \lambda v'$, we need to satisfy the following two equations:

$$(n_1 - 1)p'_1 + n_2q'a = \lambda \tag{4}$$

$$n_1q' + (n_2 - 1)p'_2a = \lambda a \tag{5}$$

These give us a quadratic equation for a:

$$a^2[n_2q'] + a[(n_1 - 1)p'_1 - (n_2 - 1)p'_2] - n_1q' = 0. \tag{6}$$

Dropping $O\left(\frac{1}{n^3}\right)$ from p'_1, p'_2, and q' and plugging into the above equation, we get:

$$a^2 \left[n_2q(1 + (1 - q)p\frac{n}{w})\right] + a \left[(n_1 - n_2)p\left(1 + (1 - p)p\frac{n}{w}\right)\right] - n_1q\left(1 + (1 - q)p\frac{n}{w}\right) = 0. \tag{7}$$

Defining $\beta = \sqrt{(n_1 - n_2)^2p^2 + 4n_1n_2q^2}$, the square root of the discriminant (Δ) of this quadratic equation is:

$$\sqrt{\Delta} = \beta\left[1 + \frac{n}{w}\frac{(n_1 - n_2)^2p^3(1 - p) + 4n_1n_2pq^2(1 - q)}{\beta^2}\right]. \tag{8}$$

We can then find the solution corresponding to $a \geq 0$:

$$a = \frac{\beta - (n_1 - n_2)p}{2n_2q} + \frac{n}{w}\frac{(n_1 - n_2)}{n_2}(p - q)p^2\frac{\beta - (n_1 - n_2)p}{2q\beta} + O\left(\frac{1}{n^3}\right). \tag{9}$$

This solution consists of two terms: The first term is exactly $\frac{EV_2}{EV_1}$ before closing a wedge. The second term is the change due to triadic closure. Since $\beta > (n_1 - n_2)p$, signs of $n_1 - n_2$ and $p - q$ determine the effect. Given group 1 is the majority group, the effect of triadic closure on a is positive if and only if $p > q$.

□

This above theorem shows that triadic closure can improve the centrality position of a minority group in an absolute sense. As above, we also examine this in a relative sense by comparing triadic closure with adding a γ-homophilous random edge.

THEOREM 2.6. *Consider the baseline of adding a γ-homophilous random edge to an SBM network G with two types consisting of n_1 and n_2 nodes, where $n_1 > n_2$. Let EV_k be the expected eigenvector centrality of a node from the kth group. For sufficiently large $n = n_1 + n_2$, triadic closure has positive relative effect on $\frac{EV_2}{EV_1}$ if and only if $\gamma > \frac{p}{q}c(p,q)$, where $c(p,q) \leq 1$. Further, $c(p,q) > \frac{q}{p}$ if $p > q$.*

See proof in Appendix A .

The proof of Theorem 2.6 follows a similar process as that of Theorem 2.5. The general idea is to approximate expected eigenvectors with eigenvectors of the expected network and then compare the change in the largest eigenvector due to adding an edge versus due to closing a wedge.

We saw in Theorem 2.6 that adding a random edge, which corresponds to $\gamma = 1$, is a hard-to-beat baseline. In a homophilous network, $\frac{p}{q}c(p,q) > 1 = \gamma$, so the relative effect is always negative. However, we can also see from this theorem that compared to a more realistic alternative ($\gamma > 1$), as long as the network is not very homophilous, i.e., $\frac{p}{q} < \gamma$, triadic closure exhibits a more favorable relative performance.

3 TRIADIC CLOSURE IN THE JACKSON-ROGERS MODEL

The Jackson-Rogers model is an evolving model originally introduced for homogeneous networks [28] and later extended to directed heterogeneous networks [9]. Here, we use an extended version of the model, which gives us more control over the incorporation of triadic closure.

The evolution of the network is defined over discrete time steps. At each step, a new node arrives and makes new connections in two phases. In the first phase, it randomly selects N_S and N_D initial friends from similar and dissimilar nodes, respectively. Note that edges are directed from the new node to the older ones. In the second phase, it chooses N_F nodes from the set of nodes accessible through an outbound edge of an initial friend. Nodes already connected to the new node are excluded from this set. This process is also biased: α proportion of these N_F nodes will be selected from the friends of the similar initial friends. The rest of the connections will be equally distributed towards the friends of the dissimilar initial friends.

In the explained Jackson-Rogers model, N_F exactly accounts for triadic closure, and we can directly control it to measure the effect while the network is evolving. This corresponds to the absolute effect. However, manipulating N_F also changes the total number of new connections per node. To distinguish the effect of triadic closure from an increased number of edges, we adopt the notion of relative effect. We say triadic closure has a positive relative effect if increasing N_F, while $N = N_S + N_D + N_F$ and $\frac{N_S}{N_D}$ are kept fixed, results in a higher network integration.

We identify homophily in the first phase of the process by $N_S > N_D$. The definition of homophily in the second phase is not straightforward as it depends on the number of friends-of-friends of different types. Our analyses in the following sections are not sensitive to the selection of α as long as $0 < \alpha < 1$.

3.1 Absolute and Relative Effects of Triadic Closure

To study the expected behavior of an evolving network from the Jackson-Rogers model, we first prove the following theorem.

THEOREM 3.1. *For an evolving Jackson-Rogers network G with K types and parameters N_S, N_D, N_F, and $1 > \alpha > \frac{1}{K}$, the network integration converges to*

$$\frac{N_D + (1 - \alpha)N_F}{N_S + N_D + \frac{K}{K-1}(1 - \alpha)N_F} \tag{10}$$

with the rate of $O\left(t^{-\frac{N_S+N_D}{N}}\right)$, regardless of the distribution of node types.

See proof in Appendix A .

In the proof of Theorem 3.1, we obtain a stronger result than the integration in equilibrium. Following Bramoullé et al. [9], we use a mean-field approximation to find a coupled differential equation of how the composition of neighbors of a node changes over time. We find a closed-form solution to this differential equation and aggregate the behavior of individual nodes to find network integration as a function of time. Understanding the dynamic of the network in time lets us study the effect of interventions in Section 3.2.

Theorem 3.1 enables us to study the effect of triadic closure on network integration in equilibrium. From this theorem, it is straightforward to see that in a network with homophily, increasing N_F, while N_S and N_D are unchanged, will increase network integration. We call this the absolute effect and formally state the observation in the following theorem.

THEOREM 3.2. *For an evolving Jackson-Rogers network G with K types and parameters N_S, N_D, N_F, and $1 > \alpha > \frac{1}{K}$, triadic closure has a positive absolute effect on network integration if and only if $N_S > \frac{N_D}{K-1}$.*

See proof in Appendix A .

As above, one might attribute the positive effect in Theorem 3.2 to the increased number of connections per node. Next, we show that even when the total number of edges per node and the composition of neighbors in the first phase are kept fixed, i.e., $N = N_S + N_D + N_F$ and $\frac{N_S}{N_D}$ are maintained, increasing N_F will improve network integration.

THEOREM 3.3. *For an evolving Jackson-Rogers network G with K types and parameters N_S, N_D, N_F, and $1 > \alpha > \frac{1}{K}$, increasing N_F subject to a fixed $N = N_S + N_D + N_F$ and $\frac{N_S}{N_D}$, results in a relative improvement in network integration if and only if $N_S > \frac{N_D}{K-1}$.*

See proof in Appendix A .

In summary, Theorems 3.2 and 3.3 show in a homophilous Jackson-Rogers evolving network, amplifying the role of triadic closure helps mitigate segregation. This effect is not due to making more connections, but rather due to the effect of triadic closure exposing nodes to dissimilar nodes.

3.2 Behavior Under a Series of Interventions

We study how interventions on a network evolving with the Jackson-Rogers model impact network integration in the short and long term. Here, we focus on interventions that act solely on the first phase. Recalling our motivating examples related to college dormitory assignments or recommendation of friendships when an individual joins an online platform, we note that an authority (i.e., university or platform, respectively) may have more leverage in this initial phase than subsequent steps which proceed through friend-of-friend searches. Such interventions that act as "nudges" in the initial phase have recently been popular in the fairness in recommender systems community; research in this space has explored the impact of bias in link formation or other selection on the long-term health of online platforms, with some work exploring the role of small nudges by the platform to mitigate inequalities or achieve other desirable social outcomes [20, 23, 26, 30, 40, 42, 43].

In our analysis of interventions, we assume that the number of links formed in the first phase is fixed. The designer has the ability to change the proportion of mono versus bichromatic edges formed in the initial seeding phase subject to this sum constraint. This intervention imitates, for instance, dorm assignments where there is a fixed number of slots per dorm, but universities have the ability to change the composition of occupants in each dorm. We also consider the setting where the designer would like to optimize network integration subject to rate-of-change constraints on the network or on the time frame over which the intervention can occur. This is a model for scenarios where it may be costly, infeasible, or undesirable to introduce a dramatic change all at once.

In the following theorem, we first find out the extent interventions can change the network integration assuming the period of intervening is very shorter than the age of the network.

THEOREM 3.4. *Let $G(T)$ be an evolving Jackson-Rogers network at time T with K types and parameters N_S, N_D, N_F, and $1 > \alpha > \frac{1}{K}$. For each $i \in [I]$, we intervene on the first phase of the evolution by setting the number of similar and dissimilar initial friends to $N_S^{(T+i)}$ and $N_D^{(T+i)}$, respectively, while the total number of initial friends is kept fixed: $N_S^{(T+i)} + N_D^{(T+i)} = N_S + N_D$. Assuming $T >> I$:*

(1) *At time $T + I$, the expected effect of ith intervention on network integration is approximately*

$$-\frac{1}{N(T+I)}\left[1 + \frac{N_F}{NT}(I-i)\frac{K\alpha-1}{K-1}\right]\Delta N_S^{(T+i)}, \tag{11}$$

where $\Delta N_S^{(T+i)} = N_S^{(T+i)} - N_S$.

(2) *At time t when a long time is passed from $T + I$ and the network is evolved with the original parameters N_S and N_D after the intervention period, the expected effect of ith intervention on network integration is approximately*

$$-\frac{1}{N}\left(\frac{t}{T}\right)^{\frac{N_F}{N}\frac{K\alpha-1}{K-1}-1}\Delta N_S^{(T+i)}. \tag{12}$$

See proof in Appendix A .

Equation 11 shows two different ways that the ith intervention changes the network: the first term in the parenthesis corresponds to the direct impact on initial friends of the node $T + i$, and the second term explains how future nodes amplify this initial effect through triadic closure. Important observations can be made from the first part of the Theorem 3.4 which are summarized in the following corollary.

Corollary 3.5. *The immediate effect of an intervention on the network of Theorem 3.4 is*

(1) *Independent of other interventions,*
(2) *Negatively proportional to the change of N_S,*
(3) *Higher if the intervention is applied earlier,*

as long as the period that interventions are applied is very shorter than the age of the network ($T >> I$).

PROOF. The first argument is obvious from Equation 11; the effect of ith intervention only depends on i. The second argument comes from the fact that $K\alpha - 1$ is always positive as α is assumed to be larger than $\frac{1}{K}$. So, the coefficient behind ΔN_S in Equation 11 is always negative. Finally, the effect of the ith intervention varies with $I - i$, so the older an intervention, the larger its effect. □

The immediate effect of interventions (Equation 11) might look in contrast to the long-term effect (Equation 12). In fact, reducing N_S has a positive impact on the number of bichromatic edges, which is sublinear in time. However, the number of total new edges is also increasing linearly over

time, and integration is the ratio of these two numbers: $\frac{sublinear(t)}{t+T}$. As we assumed the network was old enough ($T >> 1$), in the short term, the relative change of the total number of edges is small, and the effect is driven by $\approx \frac{sublinear(t)}{T}$. However, in the long term, the change in the total number of edges is not negligible, and network integration follows $\approx \frac{sublinear(t)}{t}$.

Now that we can predict the expected effect an intervention has on the network, we can design optimum interventions to maximize network integration. However, there are always some constraints, e.g., the stability of the network, that limit the change a network can tolerate. We model all of these constraints as a limit on the rate of the change. The next theorem shows there is a greedy solution for optimum interventions subject to this constraint.

THEOREM 3.6. *The optimum interventions of Theorem 3.4 such that*

$$\max_{\{N_S^{(T+j)}\}_{j \in [I]}} f(T+I)$$
$$s.t. \ \forall j \in [I-1] : f(T+j+1) - f(T+j) \leq \Delta,$$

where $f(t)$ is network integration at time t, can be found greedily from:

$$\Delta N_S^{(T+j)} = \max \left\{ -N_S, -NT\Delta\left(\frac{T}{T-j}\right) + \left[1 - \frac{N_F}{N}\frac{K\alpha - 1}{K-1}\right]\frac{1}{T-j}\sum_{i=1}^{j-1}\Delta N_S^{(T+i)} \right\}. \tag{13}$$

If $N_S \geq NT\Delta(\frac{T}{T-2I})$, there is a closed-form solution for optimum interventions during $j \in [I]$:

$$\Delta N_S^{(T+j)} = -NT\Delta\left(1 + \frac{1}{T} - \frac{N_F}{NT}\frac{K\alpha - 1}{K-1}\right)^{j-1}. \tag{14}$$

These interventions achieve $f(T+I) - f(T) = I\Delta$.

PROOF. Equation 11 can be expanded to the first order of $\frac{1}{T}$ as:

$$-\frac{1}{NT}\left[1 + \frac{N_F}{NT}(I-i)\frac{K\alpha - 1}{K-1} - \frac{I}{T}\right]\Delta N_S^{(T+i)}. \tag{15}$$

The change of integration from time $T+j-1$ to $T+j$ due to an intervention at time $T+i$ ($i < j$) is

$$\frac{1}{NT^2}\left[\frac{N_F}{N}\frac{K\alpha - 1}{K-1} - 1\right](-\Delta N_S^{(T+i)}), \tag{16}$$

where we simply found the difference of Equation 15 for $I = j$ and $I = j - 1$. Now we can rewrite the rate of the change constraint from time $T+j-1$ to $T+j$ as:

$$\frac{1}{NT}[1 - \frac{j}{T}](-\Delta N_S^{(T+j)}) + \sum_{i=1}^{j-1}\frac{1}{NT^2}\left[\frac{N_F}{N}\frac{K\alpha - 1}{K-1} - 1\right](-\Delta N_S^{(T+i)}) \leq \Delta. \tag{17}$$

This is a linear constraint in terms of $\{\Delta N_S^{(T+i)}\}_i$. The objective function is also linear:

$$f(T+I) = \frac{1}{NT}\sum_{j=1}^{I}\left[1 + \frac{N_F}{NT}(I-j)\frac{K\alpha - 1}{K-1} - \frac{I}{T}\right](-\Delta N_S^{(T+j)}) = \sum_{j=1}^{I}c_j(-\Delta N_S^{(T+j)}). \tag{18}$$

Here c_j is positive and decreasing in j. Let $-\Delta N_S^{(T+j)} = x_j$ ($j \in [I]$) be the optimum solution of the problem. We argue that for any $j \in [I]$, x_j is

$$\min\left\{N_S, NT\Delta(\frac{T}{T-j}) + \left[1 - \frac{N_F}{N}\frac{K\alpha - 1}{K-1}\right]\frac{1}{T-j}\sum_{i=1}^{j-1}x_i\right\}. \tag{19}$$

Otherwise, we could increase x_j to make the constraint of Equation 17 binding. This increase does not violate other constraints, since $\frac{N_F}{N}\frac{K\alpha - 1}{K-1} - 1 < 0$.

Now if $N_S \geq NT\Delta(\frac{T}{T-2I})$, we have

$$NT\Delta(\frac{T}{T-j}) + \left[1 - \frac{N_F}{N}\frac{K\alpha - 1}{K - 1}\right]\frac{1}{T - j}\sum_{i=1}^{j-1} x_i \leq NT\Delta(\frac{T}{T - I}) + N_S\frac{I}{T - I} \leq N_S. \tag{20}$$

So, $x_j \leq N_S$ is never binding and $x_j \approx NT\Delta + \left[1 - \frac{N_F}{N}\frac{K\alpha-1}{K-1}\right]\frac{1}{T}\sum_{i=1}^{j-1} x_i$ for all $j \in [I]$. This is a recursive equation for x_j. Let's define $y_j = \sum_{i=1}^{j} x_j$. The recursive definition for y_j will be:

$$y_j - y_{j-1} = NT\Delta + \frac{1}{T}\left[1 - \frac{N_F}{N}\frac{K\alpha - 1}{K - 1}\right]y_{j-1} \tag{21}$$

and $y_1 = x_1 = NT\Delta$. Taking Z-Transform from this recursive equation gives

$$Y(z) = \frac{NT\Delta z^{-1}}{(1 - z^{-1})(1 - (1 + \frac{1}{T} - \frac{N_F}{NT}\frac{K\alpha-1}{K-1})z^{-1})}. \tag{22}$$

By taking Z^{-1}-transform of $Y(Z)$ one can see

$$y_j = \frac{NT\Delta}{\frac{1}{T} - \frac{N_F}{NT}\frac{K\alpha-1}{K-1}}\left[(1 + \frac{1}{T} - \frac{N_F}{NT}\frac{K\alpha - 1}{K - 1})^j - 1\right], \quad j \geq 1 \tag{23}$$

and Equation 14 can be obtained by $\Delta N_S^{(T+j)} = -x_j = y_{j-1} - y_j$.

□

4 TRIADIC CLOSURE IN A FIXED-NODE EVOLVING MODEL

Asikainen et al. [5] propose a model with a fixed number of nodes and edges where the network evolves through random edge addition and triadic closure. The authors argue that triadic closure increases observed homophily relative to homophilous random link formation, i.e., triadic closure has a negative relative effect.

Here, we show that this result is specific to their definition of triadic closure which favors monochromatic wedges. In contrast, triadic closure is often studied in settings where wedges do not exhibit such a bias [19]. Empirical work on real-world networks also supports this unbiased wedge closing assumption [31]. We therefore study a variant of the Asikainen et al. [5] model where triadic closure does not differentiate between monochromatic and bichromatic wedges.

We first present the model: Consider a network with a random initial structure and where nodes belong to one of two groups. At each iteration, a *focal node* is selected uniformly at random. Then a *candidate node* is chosen by triadic closure with probability c or uniformly at random with probability $1 - c$. The parameter c controls the relative impact of triadic closure in the evolution of the network. Let θ be the focal node type and θ' be the candidate node type. A link is formed between focal and candidate nodes with probability $S'_{\theta,\theta'}$ if the candidate is selected by triadic closure and $S_{\theta,\theta'}$ otherwise. Following Asikainen et al. [5], we assume $S_{\theta,\theta'} = s$ and $S'_{\theta,\theta'} = s'$ if $\theta = \theta'$, and $S_{\theta,\theta'} = 1 - s$ and $S'_{\theta,\theta'} = 1 - s'$ otherwise. To keep the number of edges constant while network is evolving, a random edge connected to the focal node is removed whenever it forms a new edge with a candidate node.

In the original model of Asikainen et al. [5], $s' = s$ and homophily is imposed by setting $s > \frac{1}{2}$. Following the definitions above, we argue setting $s' = s$ adds extra homophily to triadic closure. Instead, to be consistent with our definition of triadic closure, we set $s' = \frac{1}{2}$. That is, we do not distinguish between monochromatic and bichromatic wedges. The result below shows how this change to an unbiased triadic closure setting leads to results consistent with observations in the SBM and Jackson-Rogers models.
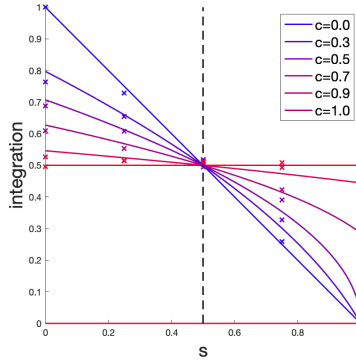
Fig. 3. Network integration obtained theoretically from the fixed-node evolving model with equiprobable types and $s' = \frac{1}{2}$. Simulation results are also marked with crosses.

Theorem 4.1. *For a fixed-node evolving network G with two equiprobable types and parameters s and $s' = \frac{1}{2}$, triadic closure has a positive relative effect on network integration if and only if $1 > s > \frac{1}{2}$, compared to a random link formation.*

See proof in Appendix A .

Note that the condition $1 > s > 1/2$ corresponds to the setting where random link formation is homophilous. To better understand the extent to which Theorem 4.1 applies, we depict network integration theoretically estimated at equilibrium in Figure 3. We have also marked simulated results with crosses to show that the theory and empirical observations closely match one another. We note that as we increase the impact of triadic closure by increasing c, integration increases if $s > \frac{1}{2}$ and decreases if $s < \frac{1}{2}$. There are two extreme cases to observe: In the case of no triadic closure ($c = 0$), integration falls linearly with respect to s. On the other extreme, when edges only form via triadic closure, i.e., $c = 1$, there are two possibilities: if groups of different types are initially completely segregated, the integration will always be zero regardless of s. If the network is not completely segregated, the resulting integration will be 0.5 as there was no homophily. Another interesting observation is that even when the network is maximally homophilous ($s = 1$), for large enough c, triadic closure will not let the integration go to zero. In sum, our above result in Theorem 4.1 and corresponding simulations show that triadic closure works against segregation in homophilous networks.

5 EXPERIMENTS

Our results so far focus on theoretical observations for the expected behavior of network properties under some approximations, for a large number of nodes, and in the limit of $t \to \infty$. In this section, we examine the validity of our results both through analysis of real data and simulations. Here we discuss the applicability of Theorem 3.1 on real data and present simulation-based evidence in Section B of the appendix.

5.1 Data: Citation Networks

The citation network we study here is known to be captured well by the Jackson-Rogers model [9, 28]. Several factors make the citation network consistent with this model: First, papers—which correspond to nodes on this graph—appear sequentially and do not disappear. Likewise, citations—which correspond to edges on this graph—are directed and do not disappear over time. Third,

Cluster	Num. of Fields	Num. of Papers	Num. of within-cluster citations
Mathematics	13	487,298	954,544
Artificial Intelligence	22	1,170,199	3,586,018
Knowledge Management	15	386,073	617,090
Electrical Engineering	20	474,773	1,172,721
Software Engineering	4	85,845	90,723
Control Engineering	7	254,453	355,930

Table 1. Summary statistics of the clusters of major fields reported.

researchers often use an initial seed of articles as a foundation for their work and use the citation network to identify further related works, similar to the second phase of the Jackson-Rogers model.

We use the network of citations extracted mainly from DBLP, ACM, and MAG (Microsoft Academic Graph) [44] (version 12). In this dataset, each paper is labeled with weighted fields of study. We use the field of study with the highest weight as the node type. The original dataset covers papers published mainly from 1960 to 2020. However, areas of study and access to articles have experienced a tremendous change during the last decades. We therefore focus on a shorter period of 2015 to 2020 to ensure network parameters are not varying over time. This period consists of more than 1.5 million articles with more than 4.7 million intra-citations, i.e., citations within the studied network.

5.2 Estimation of Model Parameters

The citation network consists of papers from various fields. We limit our analysis to major fields of study, which we define to be fields that appear in at least 1 percent of articles. Only 3 percent of papers are not related to any major field.

Despite the growth of interdisciplinary works, different fields of study still follow different publication traditions, resulting in different model parameters. We therefore first cluster the fields of study and then fit a separate model on each cluster, neglecting inter-cluster citations. Variation across clusters also provides further ability to test the validity of our theoretical findings.

Clustering Fields of Study. In order to cluster fields, we obtain a weighted graph over major fields: Nodes correspond to fields in this graph and the weight of edge (f_1, f_2) corresponds to how many times a paper in field f_1 has cited another paper with field f_2 or vice versa. Note that papers may have more than one field of study. We then use spectral clustering to obtain clusters of major fields. Here we selected the number of clusters to be 6 based on the eigenvalues of the graph's Laplacian matrix. Table 1 shows some statistics of these clusters. We chose the names of the clusters, looking at their most frequent fields.

Estimation of Each Cluster's Model Parameters. Assuming the network evolves according to the Jackson-Rogers model, we want to estimate model parameters from data. These parameters include N_S, N_D, N_F, and α. To account for the randomness of real data, we add extra randomness
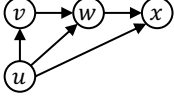
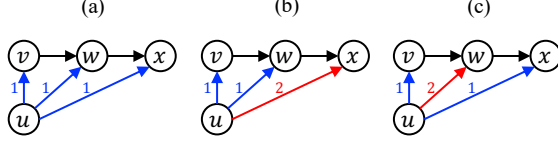Fig. 4. An example graph consists of u and $G(u)$.

Fig. 5. All feasible assignments for the edges from u to $G(u)$. The numbers on the edges indicate the phase of edge formation.

here: at each time step, when a new node u arrives, it draws model parameters from

$$N_S^{(u)} \sim \exp\left(\frac{1}{n_s}\right)$$

$$N_D^{(u)} \sim \exp\left(\frac{1}{n_d}\right)$$

$$N_{F,S}^{(u)} = \alpha^{(u)} N_F^{(u)} \sim \exp\left(\frac{1}{n_{f,s}}\right)$$

$$N_{F,D}^{(u)} = \left(1 - \alpha^{(u)}\right) N_F^{(u)} \sim \exp\left(\frac{1}{n_{f,d}}\right). \tag{24}$$

Here $\exp(\lambda)$ corresponds to an exponential distribution with mean $\frac{1}{\lambda}$. We chose exponential priors only for simplicity. We believe similar results can be obtained with other positive distributions as well. Our goal is to estimate $\theta = (n_s, n_d, n_{f,s}, n_{f,d})$.

In order to estimate θ, we need to distinguish edges created during phase one and phase two. Let $G(u) = (\mathcal{V}(u), \mathcal{E}(u))$ be the induced subgraph of the citation graph over node (paper) u's immediate descendants. Note, $G(u)$ does not include u. We want to know among all the edges from u to $\mathcal{V}(u)$ which ones are formed in the first and second phases. There is no way to distinguish first and second-phase connections. Bramoullé et al. [9] suggest that if $(v, w) \in \mathcal{E}(u)$, then (u, v) is formed initially and (u, w) is formed in the second phase due to triadic closure. However, we believe this assumption will add a bias to our estimation from model parameters. It is also not clear how to decide when there is a third node x such that $(w, x) \in \mathcal{E}(u)$ (Figure 4). We propose an approach to estimate model parameters with minimum assumptions in the following.

Let $\phi_u : \mathcal{V}(u) \rightarrow \{1, 2\}$ be the *phase assignment function* for node u. $\phi_u(v)$ determines whether (u, v) is created at the first or second phase. We call a phase assignment function *feasible* if for every $w \in \mathcal{V}(u)$ such that $\phi_u(w) = 2$, there exists a $v \in \mathcal{V}(u)$ such that $(v, w) \in \mathcal{E}(u)$ and $\phi_u(v) = 1$. In other words, if (u, w) is assigned to be shaped in the second phase, there should be at least one mediator node that u could find w through it. Figure 5 shows an example of all feasible assignments of a graph with four nodes.

Given an assignment function and a $type(\cdot)$ function, it is straightforward to find first phase parameters for node u:

$$n_s^{(u)}(\phi_u) = |\{v \in \mathcal{V}(u) \mid \phi_u(v) = 1, type(u) = type(v)\}| \tag{25}$$

$$n_d^{(u)}(\phi_u) = |\{v \in \mathcal{V}(u) \mid \phi_u(v) = 1, type(u) \neq type(v)\}|. \tag{26}$$

However, suppose an edge like (u, w) is formed in phase two, and w has immediate ancestors in $G(u)$ with both similar and dissimilar types to u. In that case, it is not clear whether u and w are connected through similar initial friends of u or dissimilar initial friends. Here we look at the ratio

of w's immediate ancestors which are similar to u and use this number as an estimate for $n_{f,s}^{(u)}$.

$$n_{f,s}^{(u)}(\phi_u) = \sum_{w:\phi_u(w)=2} \frac{|\{v \in \mathcal{V}(u) \mid (v,w) \in \mathcal{E}(u), \phi_u(v) = 1, type(v) = type(u)\}|}{|\{v \in \mathcal{V}(u) \mid (v,w) \in \mathcal{E}(u), \phi_u(v) = 1\}|} \quad (27)$$

We can do the same for ancestors which are dissimilar to u to estimate $n_{f,d}^{(u)}$:

$$n_{f,d}^{(u)}(\phi_u) = \sum_{w:\phi_u(w)=2} \frac{|\{v \in \mathcal{V}(u) \mid (v,w) \in \mathcal{E}(u), \phi_u(v) = 1, type(v) \neq type(u)|\}}{|\{v \in \mathcal{V}(u) \mid (v,w) \in \mathcal{E}(u), \phi_u(v) = 1\}|} \quad (28)$$

Let Φ_u denote the set of all feasible assignments for node u. We assume a uniform distribution over Φ_u. We can now find the likelihood of observing $G(u)$ given $\theta = (n_s, n_d, n_{f,s}, n_{f,d})$:

$$l_u(\theta) = \frac{1}{|\Phi_u|} \sum_{\phi_u \in \Phi_u} \frac{1}{n_s \, n_d \, n_{f,s} \, n_{f,d}} \exp\left(- \frac{n_s^{(u)}(\phi_u)}{n_s} - \frac{n_d^{(u)}(\phi_u)}{n_d} - \frac{n_{f,s}^{(u)}(\phi_u)}{n_{f,s}} - \frac{n_{f,d}^{(u)}(\phi_u)}{n_{f,d}} \right) \quad (29)$$

Finally, we maximize the likelihood of observing the whole cluster as it is to find the optimum parameters:

$$\theta^* = \arg\max_\theta \sum_u \log\left(l_u(\theta)\right). \quad (30)$$

We use the BFGS algorithm for the optimization; note, however, that this is a non-convex problem, and there is no guarantee that we can find the global maximum.
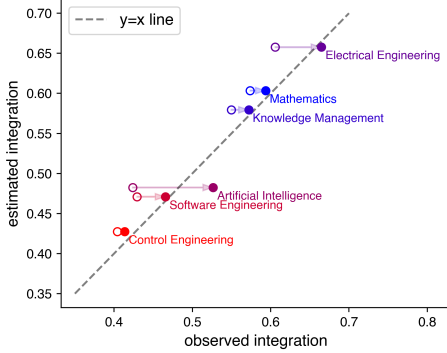

Fig. 6. Estimated vs. observed integration. Theorem 3.1 is used to estimate network integration for different clusters. Empty and filled circles correspond to beginning and end year of the study, respectively.
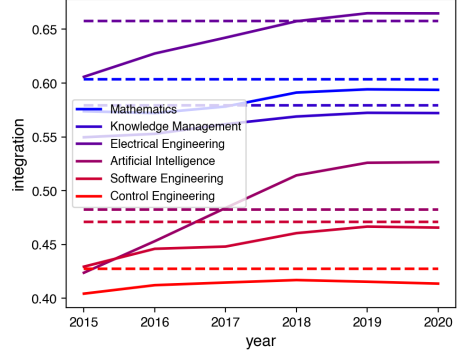
Fig. 7. Convergence behavior of observed integration (solid) to estimated integration (dashed). With the exception of one field (Artificial Intelligence), network integration in other fields has converged to the predicted value.

5.3 Results of Citation Network Analysis

We use the obtained optimum parameters θ^* and Theorem 3.1 to estimate network integration in equilibrium. Figure 6 shows the estimated integration in equilibrium versus the observed integration. In this figure, empty and filled marks correspond to the starting year (2015) and final year (2020) respectively. With the exception of one cluster (Artificial Intelligence), different clusters consistently approach our estimated values from equilibrium. The convergence behavior is also depicted in

Figure 7. These empirical insights show that even with the assumptions needed for Theorem 3.1, the theoretical insights closely match practice in this dataset. As we see from Figure 6, although clusters have various fields with different frequencies, their behavior in equilibrium is well-predicted from the theory with only a few parameters. Our empirical findings present further evidence that the Jackson-Rogers model explains citation network evolution. Finally, with estimated parameters, we find triadic closure to be responsible for 3-5% of network integration. We do so by setting $N_F = 0$ in Theorem 3.1, as a proxy for network integration without triadic closure.

6 FURTHER RELATED WORKS

Homophily is a robust and prevalent process impacting network formation in many domains [33, 36, 37]. There is a long line of theoretical and empirical work exploring the effect of homophily on network formation, ranging from observational studies on large network data, to laboratory experiments, to analyses of theoretical models [3, 17, 21].

A main topic of focus has been the interaction between homophily and network segregation. For instance, Currarini et al. [13], Henry et al. [25] show that segregated networks emerge due to homophily. In related work, Kim and Altmann [29] study the effect of homophily on the rich-get-richer phenomena. Empirical work has explored the effect of homophily on integration in settings like college campuses [34]. In related work to ours, Bramoullé et al. [9] adapt the Jackson-Rogers model to the case with heterogeneous nodes. Their work primarily focuses on how each node's likelihood to form links changes over time. In contrast, we consider a global measurement of integration, using the fraction of bichromatic edges.

Triadic closure is another well-studied process in network formation dating back to the 1950s [31, 39]. While there is a long line of work on the effect of triadic closure on network clustering, the interplay between homophily and triadic closure remains under-explored. In one complementary related work, Altenburger and Ugander [4] show that monophily—the presence of individuals with preference for attributes unrelated to their own—has a tendency to induce similarity among friends-of-friends. In contrast, we study the relationship of homophily and triadic closure, though some of the findings complement our observations.

The closest work to ours is that by Asikainen et al. [5], which explores the interaction of triadic closure and homophily. Here, we are similarly concerned with how these two phenomena interact in dynamic models. Asikainen et al. [5] consider a model that also starts with an SBM and adds both triadic closure and random link rewiring. Both of these additions are influenced by choice homophily. Under this model, Asikainen et al. [5] show that triadic closure amplifies the effects of homophily. We note, however, the model considered here already has the triadic closure step influenced by homophily. In our work, we make minimal adjustments to their model to further isolate the effects of triadic closure and find results consistent with the SBM and Jackson-Rogers models.

Segregation in social networks can limit individuals' ability to access information, resources, and opportunities, leading to the creation or exacerbation of disparities across groups. Research across various disciplines has modeled and measured the impact of segregation on social welfare including its impacts on access to information, economic development, educational outcomes, labor market outcomes, and social capital and support [7, 10, 11, 14, 16, 18, 27] Recent work, such as by Avin et al. [6] has proposed and studied models that explain how inequality and disparities in access to opportunity arise in certain settings.

Our work has additional implications for network-based interventions both in on- and off-line settings. For instance, it is well-known that biases that may exist on online platforms such as Twitter and Task Rabbit may lead to inequalities between groups [24, 38]. These biases, amplified by recommendation algorithms, can impact how networks grow and evolve creating an *algorithmic*

glass ceiling [8, 8, 42, 43]. In recent years, there has been interest by researchers in algorithmically-informed interventions that can help better diagnose and mitigate underlying patterns of inequality on platforms [1, 2]. Focused on fairness in recommender systems, researchers have examined the effect of small interventions on the long-term health of the platform such as by mitigating segregation, improving interactions, and achieving other desirable societal objectives [20, 23, 26, 30, 40, 42, 43]. These studies have shown that the platform designer, by using small interventions when a user first joins, may be able to realize large gains on the platform health over time.

7 DISCUSSION AND CONCLUSION

In this work, we consider the effect of triadic closure on network segregation. Through analyses of different static and dynamic network formation models, we find that triadic closure has the effect of increasing network integration, indicating that it may be a process that counteracts homophily in network formation.

We find it striking that such a tension should exist between two such well-studied social processes as homophily and triadic closure. In addition to the theoretical and empirical results tackled in this work, we believe this counter-intuitive result about the relationship between homophily and triadic closure points to a rich and under-explored phenomenon about their interaction.

These results also open up questions related to other measurements of network health, such as network expansion and distribution of network centralities. Each of these points to challenging analytic questions. Empirically, it would also be interesting to shed light on what types of social and information networks tend to exhibit a stronger relationship between triadic closure and homophily.

Finally, the interventions presented in this work point to a broader set of theoretical and empirical questions. For instance, it would be interesting to estimate the various network parameters and compare the effect of nudges across different distributions of values. Furthermore, such interventions are often costly to the designer or may incur social cost, leading to a set of optimization questions where the designer must trade off these costs with utility gained from network integration.

ACKNOWLEDGMENTS

REFERENCES

[1] Rediet Abebe, Solon Barocas, Jon Kleinberg, Karen Levy, Manish Raghavan, and David G Robinson. 2020. Roles for computing in social change. In *Proceedings of the 2020 Conference on Fairness, Accountability, and Transparency*. 252–260.

[2] Rediet Abebe and Kira Goldner. 2018. Mechanism design for social good. *AI Matters* 4, 3 (2018), 27–34.

[3] Lada A Adamic and Natalie Glance. 2005. The political blogosphere and the 2004 US election: divided they blog. In *Proceedings of the 3rd international workshop on Link discovery*. 36–43.

[4] Kristen M Altenburger and Johan Ugander. 2018. Monophily in social networks introduces similarity among friends-of-friends. *Nature human behaviour* 2, 4 (2018), 284.

[5] Aili Asikainen, Gerardo Iñiguez, Javier Ureña-Carrión, Kimmo Kaski, and Mikko Kivelä. 2020. Cumulative effects of triadic closure and homophily in social networks. *Science Advances* 6, 19 (2020), eaax7310.

[6] Chen Avin, Barbara Keller, Zvi Lotker, Claire Mathieu, David Peleg, and Yvonne-Anne Pignolet. 2015. Homophily and the glass ceiling effect in social networks. In *Proceedings of the 2015 conference on innovations in theoretical computer science*. 41–50.

[7] Abhijit Banerjee, Arun G Chandrasekhar, Esther Duflo, and Matthew O Jackson. 2013. The diffusion of microfinance. *Science* 341, 6144 (2013).

[8] Asia J Biega, Krishna P Gummadi, and Gerhard Weikum. 2018. Equity of Attention: Amortizing Individual Fairness in Rankings. *arXiv preprint arXiv:1805.01788* (2018).

[9] Yann Bramoullé, Sergio Currarini, Matthew O Jackson, Paolo Pin, and Brian W Rogers. 2012. Homophily and long-run integration in social networks. *Journal of Economic Theory* 147, 5 (2012).

[10] Antoni Calvo-Armengol and Matthew O Jackson. 2004. The effects of social networks on employment and inequality. *American Economic Review* 94, 3 (2004).

[11] Antoni Calvo-Armengol, Eleonora Patacchini, and Yves Zenou. 2009. Peer effects and social networks in education. *The Review of Economic Studies* 76, 4 (2009).

[12] Fan Chung and Mary Radcliffe. 2011. On the spectra of general random graphs. *the electronic journal of combinatorics* (2011), P215–P215.

[13] Sergio Currarini, Matthew O Jackson, and Paolo Pin. 2009. An economic model of friendship: Homophily, minorities, and segregation. *Econometrica* 77, 4 (2009), 1003–1045.

[14] Krishna Dasaratha. 2017. Distributions of Centrality on Networks. *arXiv preprint arXiv:1709.10402* (2017).

[15] Michela Del Vicario, Gianna Vivaldo, Alessandro Bessi, Fabiana Zollo, Antonio Scala, Guido Caldarelli, and Walter Quattrociocchi. 2016. Echo chambers: Emotional contagion and group polarization on facebook. *Scientific reports* 6, 1 (2016), 1–12.

[16] Paul DiMaggio and Filiz Garip. 2011. How network externalities can exacerbate intergroup inequality. *Amer. J. Sociology* 116, 6 (2011), 1887–1933.

[17] Yuxiao Dong, Reid A Johnson, Jian Xu, and Nitesh V Chawla. 2017. Structural diversity and homophily: A study across more than one hundred big networks. In *Proceedings of the 23rd ACM SIGKDD International Conference on Knowledge Discovery and Data Mining*. 807–816.

[18] Nathan Eagle, Michael Macy, and Rob Claxton. 2010. Network diversity and economic development. *Science* 328, 5981 (2010), 1029–1031.

[19] David Easley and Jon Kleinberg. 2010. *Networks, Crowds, and Markets: Reasoning about a Highly Connected World*. Cambridge University Press. https://doi.org/10.1017/CBO9780511761942

[20] Michael D Ekstrand and Martijn C Willemsen. 2016. Behaviorism is not enough: better recommendations through listening to users. In *Proceedings of the 10th ACM Conference on Recommender Systems*. ACM, 221–224.

[21] Jacob K Goeree, Arno Riedl, and Aljaž Ule. 2009. In search of stars: Network formation among heterogeneous agents. *Games and Economic Behavior* 67, 2 (2009).

[22] Mark S Granovetter. 1977. The strength of weak ties. In *Social networks*. Elsevier, 347–367.

[23] Ido Guy. 2015. Social recommender systems. In *Recommender Systems Handbook*. Springer, 511–543.

[24] Anikó Hannák, Claudia Wagner, David Garcia, Alan Mislove, Markus Strohmaier, and Christo Wilson. 2017. Bias in online freelance marketplaces: Evidence from taskrabbit and fiverr. In *Proceedings of the 2017 ACM conference on computer supported cooperative work and social computing*. 1914–1933.

[25] Adam Douglas Henry, Paweł Prałat, and Cun-Quan Zhang. 2011. Emergence of segregation in evolving social networks. *Proc. of the National Academy of Sciences* 108, 21 (2011).

[26] Jevan Hutson, Jessie G Taft, Solon Barocas, and Karen Levy. 2018. Debiasing Desire: Addressing Bias & Discrimination on Intimate Platforms. *arXiv preprint arXiv:1809.01563* (2018).

[27] Matthew O. Jackson, Tomas Rodriguez-Barraquer, and Xu Tan. 2012. Social Capital and Social Quilts: Network Patterns of Favor Exchange. *American Economic Review* 102, 5 (May 2012). https://doi.org/10.1257/aer.102.5.1857

[28] Matthew O. Jackson and Brian W. Rogers. 2007. Meeting Strangers and Friends of Friends: How Random Are Social Networks? *American Economic Review* 97, 3 (June 2007), 890–915. https://doi.org/10.1257/aer.97.3.890

[29] Kibae Kim and Jörn Altmann. 2017. Effect of homophily on network formation. *Comm. in Nonlinear Science and Numerical Simulation* 44 (2017).

[30] Bart P Knijnenburg, Saadhika Sivakumar, and Daricia Wilkinson. 2016. Recommender systems for self-actualization. In *Proceedings of the 10th ACM Conference on Recommender Systems*. ACM, 11–14.

[31] Gueorgi Kossinets and Duncan J Watts. 2006. Empirical analysis of an evolving social network. *science* 311, 5757 (2006), 88–90.

[32] Gueorgi Kossinets and Duncan J Watts. 2009. Origins of homophily in an evolving social network. *American journal of sociology* 115, 2 (2009), 405–450.

[33] Paul F Lazarsfeld, Robert K Merton, et al. 1954. Friendship as a social process: A substantive and methodological analysis. *Freedom and control in modern society* 18, 1 (1954), 18–66.

[34] Adalbert Mayer and Steven L Puller. 2008. The old boy (and girl) network: Social network formation on university campuses. *Journal of Public Economics* 92, 1-2 (2008).

[35] J Miller McPherson and Lynn Smith-Lovin. 1987. Homophily in voluntary organizations: Status distance and the composition of face-to-face groups. *American sociological review* (1987), 370–379.

[36] Miller McPherson, Lynn Smith-Lovin, and James M Cook. 2001. Birds of a feather: Homophily in social networks. *Annual review of sociology* 27, 1 (2001).

[37] Mark EJ Newman. 2002. Assortative mixing in networks. *Physical review letters* 89, 20 (2002), 208701.

[38] Shirin Nilizadeh, Anne Groggel, Peter Lista, Srijita Das, Yong-Yeol Ahn, Apu Kapadia, and Fabio Rojas. 2016. Twitter's glass ceiling: The effect of perceived gender on online visibility. In *Proceedings of the International AAAI Conference on Web and Social Media*, Vol. 10. 289–298.

[39] Anatol Rapoport. 1953. Spread of information through a population with socio-structural bias: I. Assumption of transitivity. *The bulletin of mathematical biophysics* 15, 4 (1953), 523–533.

[40] Tobias Schnabel, Paul N Bennett, Susan T Dumais, and Thorsten Joachims. 2018. Short-term satisfaction and long-term coverage: Understanding how users tolerate algorithmic exploration. In *Proceedings of the Eleventh ACM International Conference on Web Search and Data Mining*. ACM, 513–521.

[41] Wesley Shrum, Neil H Cheek Jr, and Saundra MacD. 1988. Friendship in school: Gender and racial homophily. *Sociology of Education* (1988), 227–239.

[42] Ana-Andreea Stoica, Christopher Riederer, and Augustin Chaintreau. 2018. Algorithmic Glass Ceiling in Social Networks: The effects of social recommendations on network diversity. In *Proceedings of the 2018 World Wide Web Conference*. 923–932.

[43] Jessica Su, Aneesh Sharma, and Sharad Goel. 2016. The effect of recommendations on network structure. In *Proceedings of the 25th international conference on World Wide Web*. 1157–1167.

[44] Jie Tang, Jing Zhang, Limin Yao, Juanzi Li, Li Zhang, and Zhong Su. 2008. ArnetMiner: Extraction and Mining of Academic Social Networks. In *KDD'08*. 990–998.

[45] Gergő Tóth, Johannes Wachs, Riccardo Di Clemente, Ákos Jakobi, Bence Ságvári, János Kertész, and Balázs Lengyel. 2019. Inequality is rising where social network segregation interacts with urban topology. *arXiv preprint arXiv:1909.11414* (2019).

[46] Dan Zeltzer. 2020. Gender homophily in referral networks: Consequences for the medicare physician earnings gap. *American Economic Journal: Applied Economics* 12, 2 (2020), 169–97.

A ADDITIONAL STATEMENTS AND PROOFS

Lemma A.1. *For any $SBM(p, q)$ network G with $K \geq 2$ types each consisting of n_k nodes ($k \in [K]$), the expected number of monochromatic edges is*

$$e_m = \sum_{k \in [K]} \binom{n_k}{2} p = \frac{1}{2} p \sum_k n_k^2 + O(n),$$

and the expected number of bichromatic edges is

$$e_b = \frac{1}{2} \sum_{k \in [K]} \sum_{l \in [K], l \neq k} n_k n_l q = \frac{1}{2} q \left(n^2 - \sum_k n_k^2\right) + O(n), \tag{31}$$

where $n = \sum_k n_k$. Further, the expected number of monochromatic missing edges is

$$o_m = \sum_{k \in [K]} \binom{n_k}{2} (1 - p) = \frac{1}{2}(1 - p) \sum_k n_k^2 + O(n),$$

and the expected number of bichromatic missing edges is

$$o_b = \frac{1}{2} \sum_{k \in [K]} \sum_{l \in [K], l \neq k} n_k n_l (1 - q) = \frac{1}{2}(1 - q) \left(n^2 - \sum_k n_k^2\right) + O(n), \tag{32}$$

where we call an edge (i, j) a missing edge if i and j are not connected in G.

PROOF. To find e_m (o_m), we sum the number of unordered pairs from each group times the probability they are connected (not connected). To find e_b (o_b), we count the number of bichromatic pairs times the probability they are connected (not connected) times $\frac{1}{2}$ to compensate for repeated counting. □

Lemma A.2. *For the same network as Lemma A.1, the expected number of monochromatic wedges is*

$$w_m = \sum_{k \in [K]} \binom{n_k}{2} (n_k - 2) p^2 (1 - p) + \sum_{k \in [K]} \binom{n_k}{2} (n - n_k) q^2 (1 - p)$$

$$= \frac{1}{2} p^2 (1 - p) \sum_k n_k^3 + \frac{1}{2} q^2 (1 - p) \left(n \sum_k n_k^2 - \sum_k n_k^3\right) + O(n^2), \tag{33}$$

and the expected number of bichromatic wedges is

$$w_b = \sum_{k \in [K]} \sum_{l \in [K], l \neq k} n_k (n_k - 1) n_l pq(1 - q) + \sum_{k \in [K]} \sum_{l \in [K], l \neq k} \frac{1}{2} n_k n_l (n - n_k - n_l) q^2 (1 - q)$$

$$= pq(1 - q) \left(n \sum_k n_k^2 - \sum_k n_k^3\right) + \frac{1}{2} q^2 (1 - q) \left(n^3 + 2 \sum_k n_k^3 - 3n \sum_k n_k^2\right) + O(n^2) \tag{34}$$

PROOF. For a wedge $i-j-k$, the first term of w_m is the expected number of wedges such that $type(i) = type(j) = type(k)$. The second term of w_m corresponds to the case $type(i) = type(k) \neq type(j)$. The first term of w_b is the expected number of wedges such that $type(i) = type(j) \neq type(k)$. The second term of w_b corresponds to the case where i, j, and k are all from different types. □

Lemma A.3. *For any set of $\{n_1, n_2, \cdots, n_K | n_i \in \mathbb{R}^+\}$, following inequalities hold:*

(1) $n^2 \geq m_2$
(2) $nm_2 \geq m_3$
(3) $nm_3 \geq m_2^2$
(4) $2m_2^2 \geq nm_3$

(5) $2nm_2^2 \geq n^2m_3 + m_2m_3$,

where $n = \sum_{k \in [K]} n_k$ and $m_i = \sum_{k \in [K]} n_k^i$.

PROOF. We start by the first inequality and use the results to that point in proving each inequality.

(1)

$$n^2 - m_2 = \sum_{i,j} n_i n_j - \sum_j n_j^2$$
$$= \sum_{i \neq j} n_i n_j \geq 0.$$

(2)

$$nm_2 - m_3 = \sum_{i,j} n_i n_j^2 - \sum_j n_j^3$$
$$= \sum_{i \neq j} n_i n_j^2 \geq 0.$$

(3)

$$nm_3 - m_2^2 = \sum_{i,j} n_i n_j^3 - n_i^2 n_j^2$$
$$= \sum_{i \neq j} n_i n_j^3 + n_j n_i^3 - 2n_i^2 n_j^2$$
$$= \sum_{i \neq j} n_i n_j (n_i - n_j)^2 \geq 0.$$

(4)

$$2m_2^2 - nm_3 = \sum_{i,j} 2n_i^2 n_j^2 - n_i n_j^3$$
$$= \sum_{i \neq j} n_i^4 + n_j^4 + 4n_i^2 n_j^2 - n_i n_j^3 - n_j n_i^3$$
$$= \sum_{i \neq j} (n_i^2 + n_j^2)^2 - n_i n_j (n_i - n_j)^2.$$

As $n_i, n_j \geq 0$, $n_i^2 + n_j^2 \geq (\max(n_i, n_j))^2 \geq n_i n_j$ and $n_i^2 + n_j^2 \geq (\max(n_i, n_j))^2 \geq (n_i - n_j)^2$. So, $(n_i^2 + n_j^2)^2 \geq n_i n_j (n_i - n_j)^2$, which gives $2m_2^2 - nm_3 \geq 0$.

(5)

$$2nm_2^2 - n^2m_3 - m_2m_3 = (\sum_{i,j} 2n_i^2n_j^2 - n_in_j^2)n - \sum_{i,j} n_i^2n_j^3$$

$$= \sum_{i\neq j}(n_i^4 + n_j^4 + 4n_i^2n_j^2 - n_in_j^3 - n_jn_i^3)n - \sum_{i\neq j} n_i^5 + n_j^5 + n_i^2n_j^3 + n_j^2n_i^3$$

$$= \sum_{i\neq j}((n_i^2 + n_j^2)^2 - n_in_j(n_i - n_j)^2)(n - n_i - n_j)$$

$$+ \sum_{i\neq j}(n_i^4 + n_j^4 + 4n_i^2n_j^2 - n_in_j^3 - n_jn_i^3)(n_i + n_j) - n_i^5 + n_j^5 + n_i^2n_j^3 + n_j^2n_i^3$$

$$\geq \sum_{i\neq j}(n_i^4 + n_j^4 + 4n_i^2n_j^2 - n_in_j^3 - n_jn_i^3)(n_i + n_j) - (n_i^5 + n_j^5 + n_i^2n_j^3 + n_j^2n_i^3)$$

$$= \sum_{i\neq k} 2n_i^2n_j^3 + 2n_j^2n_i^2 \geq 0.$$

Here we used $(n_i^2 + n_j^2)^2 - n_in_j(n_i - n_j)^2 \geq 0$ from the proof of the previous part.

$\square$

Lemma A.4. *Let A be a $K \times K$ real symmetric matrix such that*

$$[A]_{i,j} = \begin{cases} c & i = j \\ \frac{1}{K-1}(1 - c) & o.w. \end{cases}. \tag{35}$$

Then, A has K real eignvalues:

$$d_i = \begin{cases} 1 & i = 1 \\ \frac{Kc-1}{K-1} & 1 < i \leq K \end{cases}, \tag{36}$$

with corresponding eigenvectors:

$$[v_1]_j = 1$$

$$For\ i \geq 2:\ [v_i]_j = \begin{cases} 1 & j = 1 \\ -1 & j = i \\ 0 & o.w. \end{cases}. \tag{37}$$

PROOF. For $i = 1$:

$$[Av_1]_j = 1 = d_1[v_1]_j. \tag{38}$$

For $1 < i \leq K$:

$$[Av_i]_j = \begin{cases} \frac{Kc-1}{K-1} & j = 1 \\ -\frac{Kc-1}{K-1} & j = i \\ 0 & o.w. \end{cases} = d_i[v_1]_j. \tag{39}$$

$\square$

Lemma A.5. *The inverse of the $K \times K$ matrix V defined by*

$$[V]_{i,j} = \begin{cases} 1 & i = 1\ or\ j = 1 \\ -1 & i = j > 1 \\ 0 & o.w. \end{cases} \tag{40}$$

is

$$[V^{-1}]_{i,j} = \begin{cases} -\frac{K-1}{K} & i = j > 1 \\ \frac{1}{K} & o.w. \end{cases}.$$

(41)

PROOF.

$$[VV^{-1}]_{i,j} = \begin{cases} 1 & i = j = 1 \\ \frac{1}{K} + \frac{K-1}{K} = 1 & i = j > 1 \\ 0 & o.w. \end{cases}.$$

(42)

□

PROOF OF THEOREM 2.1. Let e_b and e_m (w_b and w_m) be the expected number of bichromatic and monochromatic edges (wedges) respectively. The expected integration of the network before modification is approximately $\frac{e_b}{e_m+e_b}$. [1] After closing a random wedge, the expected (network) integration will be approximately $\frac{e_b+w_b/(w_m+w_b)}{e_m+e_b+1}$. For a fixed p, we are looking for the range of q which increases the current level of integration:

$$\frac{e_b + w_b/(w_m + w_b)}{e_m + e_b + 1} \geq \frac{e_b}{e_m + e_b}$$

$$\Longleftrightarrow e_m e_b + e_b^2 + \frac{w_b}{w_m + w_b}(e_m + e_b) \geq e_m e_b + e_b^2 + e_b$$

$$\Longleftrightarrow \frac{w_b}{w_m} \geq \frac{e_b}{e_m}.$$

(43)

Let's define $n = \sum_{k \in [K]} n_k$ and $m_i = \sum_{k \in [K]} n_k^i$. By plugging e_m, e_b, w_m, and w_b from Lemmas A.1 and A.2 into the above inequality:

$$\frac{w_b}{w_m} = \frac{(1-q)q}{1-p} \frac{2p(nm_2 - m_3) + q(n^3 + 2m_3 - 3nm_2)}{p^2 m_3 + q^2(nm_2 - m_3)} \geq \frac{q}{p} \frac{n^2 - m_2}{m_2} = \frac{e_b}{e_m}$$

$$\Longleftrightarrow q^2 \Big[-(1-p)(n^2 - m_2)(nm_2 - m_3) - pm_2\big(n(n^2 - m_2) - 2(nm_2 - m_3)\big) \Big] +$$

$$qp \Big[-2(1+p)m_2(nm_2 - m_3) + nm_2(n^2 - m_2) \Big] +$$

$$p^2 \Big[2m_2(nm_2 - m_3) - (1-p)m_3(n^2 - m_2) \Big] \geq 0.$$

(44)

Here we used the fact that $nm_2 \geq m_3$ from Lemma A.3. To determine the feasible region of q we have to find the roots of LHS of Equation 44 which is a quadratic function in q. Let's define three new variables to simplify the equations: $A = n^2 - m_2$, $B = nm_2 - m_3$, and $C = m_3 A - m_2 B = n(nm_3 - m_2^2)$. According to Lemma A.3, A, B, and C are all non-negative variables. The discriminant (Δ) of the

---

[1] We approximated $\mathbb{E}[\frac{num}{den}]$ by $\frac{\mathbb{E}[num]}{\mathbb{E}[den]}$.

quadratic function can be found:

$$
\begin{aligned}
\frac{\Delta}{p^2} &= m_2^2(-2(1+p)B + nA)^2 + 4\big[(1-p)AB + pm_2(nA - 2B)\big]\big[2m_2B - (1-p)m_3A\big] \\
&= m_2^2(-2(1-p)B + nA)^2 + 8m_2(1-p)AB^2 - 4(1-p)^2m_3A^2B - p(1-p)m_2m_3(nA - 2B)A \\
&= (1-p)^2\big[4m_2^2B^2 - 4m_3A^2B + 4m_2m_3(nA - 2B)A\big] \\
&\quad + (1-p)\big[-4nm_2^2AB + 8m_2AB^2 - 4m_2m_3A(nA - 2B)\big] \\
&\quad + n^2m_2^2A^2 \\
&= 4(1-p)^2C^2 - 4(1-p)nm_2AC + n^2m_2^2A^2 \\
&= \big(nm_2A - 2(1-p)C\big)^2.
\end{aligned}
\tag{45}
$$

As $\Delta > 0$, the quadratic has always two real roots:

$$
\begin{aligned}
q_1^*, q_2^* &= \frac{p}{2}\frac{2(1+p)m_2B - nm_2A \pm \sqrt{\Delta}}{-(1-p)AB - pm_2(nA - 2B)} \\
&= \frac{p}{2}\frac{2(1-p)(-m_2B) + 4m_2B - nm_2A \pm (nm_2A - 2(1-p)C)}{(1-p)(-AB + nm_2A - 2m_2B) - m_2(nA - 2B)} \\
&= p\frac{(1-p)(-m_2B - \pm C) + m_2\big(2B - \frac{nA}{2}(1 - \pm 1)\big)}{(1-p)(C - m_2B) + m_2(2B - nA)} \\
&= p,\ p\frac{-(1-p)m_3A + 2m_2B}{(1-p)(C - m_2B) + m_2(2B - nA)}.
\end{aligned}
\tag{46}
$$

The first root is always $q_1^* = p$ regardless of the network's structure. For the numerator of the second root, q_2^*, we have:

$$
\begin{aligned}
-(1-p)m_3A + 2m_2B &\geq 2m_2B - m_3A \\
&= 2m_2(nm_2 - m_3) - m_3(n^2 - m_2) \\
&= 2nm_2^2 - n^2m_3 - m_2m_3 \geq 0,
\end{aligned}
\tag{47}
$$

where we applied Lemma A.3 to obtain the final inequality. Further, plugging $2m_2B \geq m_3A$ into the denominator of q_2^* gives:

$$
\begin{aligned}
(1-p)(C - m_2B) + m_2(2B - nA) &= (1-p)(m_3A - 2m_2B) + m_2(2B - nA) \\
&\leq m_2(2B - nA) \\
&= m_2(2(nm_2 - m_3) - n(n^2 - m_2)) \\
&= m_2(n(m_2 - n^2) - 2m_3) \\
&\leq m_2 - n^2 \leq 0,
\end{aligned}
\tag{48}
$$

where we used Lemma A.3 to obtain the last inequality. Note that the denominator of q_2^* is exactly the coefficient of q^2 in the quadratic function of Equation 44. So, Equation 48 says that this quadratic function is concave. On the other hand, Equations 47 and 48 shows $q_2^* \leq 0$. So, we can conclude that the inequality of Equation 44 holds if and only if $q_2^* \leq 0 \leq q \leq q_1^* = p$.

□

PROOF OF THEOREM 2.2. Let e_b, e_m, o_b, o_m, w_b, and w_m be the expected number of bichromatic edges, monochromatic edges, bichromatic missing edges, monochromatic missing edges, bichromatic wedges, and monochromatic wedges, respectively. After closing a random wedge, the expected

integration will be approximately $\frac{e_b + w_b/(w_m + w_b)}{e_m + e_b + 1}$. Similarly, after adding a random edge, the expected integration will be approximately $\frac{e_b + o_b/(o_m + o_b)}{e_m + e_b + 1}$. For a fixed q, we are looking for the range of p such that closing a random wedge increases network integration more than adding a random edge:

$$\frac{e_b + w_b/(w_m + w_b)}{e_m + e_b + 1} \geq \frac{e_b + o_b/(o_m + o_b)}{e_m + e_b + 1}$$

$$\iff \frac{w_b}{w_m + w_b} \geq \frac{o_b}{o_m + o_b}$$

$$\iff \frac{w_b}{w_m} \geq \frac{o_b}{o_m}. \tag{49}$$

Let's define $n = \sum_{k \in [K]} n_k$ and $m_i = \sum_{k \in [K]} n_k^i$. By plugging o_m, o_b, w_m, and w_b from Lemmas A.1 and A.2 into the above inequality:

$$\frac{w_b}{w_m} = \frac{(1-q)q}{1-p} \frac{2p(nm_2 - m_3) + q(n^3 + 2m_3 - 3nm_2)}{p^2 m_3 + q^2(nm_2 - m_3)} \geq \frac{(1-q)}{(1-p)} \frac{n^2 - m_2}{m_2} = \frac{o_b}{o_m}$$

$$\iff p^2 \left[-m_3(n^2 - m_2) \right] +$$

$$pq \left[2m_2(nm_2 - m_3) \right] +$$

$$q^2 \left[nm_2(n^2 - m_2) - 2m_2(nm_2 - m_3) - (n^2 - m_2)(nm_2 - m_3) \right] \geq 0. \tag{50}$$

Here we used the fact that $nm_2 \geq m_3$ from Lemma A.3. To determine the feasible region of p we have to find the roots of LHS of Equation 50 which is a quadratic function in p. Let's define three new variables to simplify the equations: $A = n^2 - m_2$, $B = nm_2 - m_3$, and $C = m_3 A - m_2 B = n(nm_3 - m_2^2)$. According to Lemma A.3, A, B, and C are all non-negative variables. The discriminant (Δ) of the quadratic function is:

$$\frac{\Delta}{4q^2} = (m_2 B)^2 + m_3 A(nm_2 A - 2m_2 B - AB)$$

$$= m_2 B^2 - 2m_2 m_3 AB + nm_2 m_3 A^2 - m_3 A^2 B$$

$$= m_2 B^2 - 2m_2 m_3 AB + m_3 A^2(nm_2 - B)$$

$$= (m_3 A - m_2 B)^2 = C^2. \tag{51}$$

As $\Delta \geq 0$, the quadratic has always two [2] real roots:

$$p_1^*, p_2^* = q \frac{-m_2 B \pm C}{-m_3 A}$$

$$= q, \ q\left(\frac{2m_2 B}{m_3 A} - 1\right). \tag{52}$$

The first root is always $p_1^* = q$ regardless of the network's structure. Expanding the ratio $\frac{2m_2 B}{m_3 A}$ appeared in the second root and applying Lemma A.3, we can see $1 \leq \frac{2m_2 B}{m_3 A} \leq 2$. So, defining $l^* = \frac{2m_2 B}{m_3 A} - 1$, we have $0 \leq p_2^* = q\, l^* \leq 1$. On the other hand, the coefficient of the p^2 term in the quadratic function of Equation 50 is always negative. Therefore, the quadratic function is concave and p satisfies the inequality of Equation 50 if and only if $q \geq p \geq q\, l^*$. As $p > q$ does not fall into this range, a direct result is that triadic closure has negative relative effect when network is homophilous.

$\square$

---

[2]Possibly degenerate.

PROOF OF THEOREM 2.4. We use the same notation as the proof of Theorem 2.2. After closing a random wedge, the expected integration will be approximately $\frac{e_b + w_b/(w_m + w_b)}{e_m + e_b + 1}$. After adding a γ-homophilous random edge, the expected integration will be approximately $\frac{e_b + o_b/(\gamma o_m + o_b)}{e_m + e_b + 1}$. For a fixed q, we are looking for the range of p such that closing a random wedge increases network integration more than adding a homophilous random edge:

$$\frac{e_b + w_b/(w_m + w_b)}{e_m + e_b + 1} \geq \frac{e_b + o_b/(\gamma o_m + o_b)}{e_m + e_b + 1}$$

$$\iff \frac{w_b}{w_m + w_b} \geq \frac{o_b}{\gamma o_m + o_b}$$

$$\iff \frac{w_b}{w_m} \geq \frac{1}{\gamma} \frac{o_b}{o_m}. \tag{53}$$

By plugging o_m, o_b, w_m, and w_b from Lemmas A.1 and A.2 into the above inequality:

$$\frac{w_b}{w_m} = \frac{(1-q)q}{1-p} \frac{2p(nm_2 - m_3) + q(n^3 + 2m_3 - 3nm_2)}{p^2 m_3 + q^2(nm_2 - m_3)} \geq \frac{1}{\gamma} \frac{(1-q)}{(1-p)} \frac{n^2 - m_2}{m_2} = \frac{1}{\gamma} \frac{o_b}{o_m}$$

$$\iff p^2 \big[-m_3 A \big] + pq \big[2\gamma m_2 B \big] + q^2 \big[\gamma n m_2 A - 2\gamma m_2 B - AB \big] \geq 0. \tag{54}$$

Here we used the fact that $nm_2 \geq m_3$ from Lemma A.3. To determine the feasible region of p, we have to find the roots of LHS of Equation 54 which is a quadratic function in p. The discriminant (Δ) of the quadratic function is:

$$\frac{\Delta}{4q^2} = (\gamma A B)^2 + m_3 A (\gamma n m_2 A - 2\gamma m_2 B - AB)$$

$$= (\gamma m_2 B)^2 - 2\gamma m_2 m_3 A B + m_3 A^2 (\gamma n m_2 - B)$$

$$= (\gamma m_2 B - m_3 A)^2 + m_3 A^2 (\gamma n m_2 - B - m_3)$$

$$= (\gamma m_2 B - m_3 A)^2 + (\gamma - 1) n m_2 m_3 A^2. \tag{55}$$

As $\Delta \geq 0$, the quadratic has always two real roots:

$$p_1^*, p_2^* = q \frac{\gamma m_2 B \pm \sqrt{(\gamma m_2 B - m_3 A)^2 + (\gamma - 1) n m_2 m_3 A^2}}{m_3 A}$$

$$= q\, u(\gamma), q\, l(\gamma). \tag{56}$$

We can bound $u(\cdot)$ by

$$u(\gamma) = \frac{\gamma m_2 B + \sqrt{(\gamma m_2 B - m_3 A)^2 + (\gamma - 1) n m_2 m_3 A^2}}{m_3 A}$$

$$\geq \frac{\gamma m_2 B + |\gamma m_2 B - m_3 A|}{m_3 A} = \begin{cases} \frac{2\gamma m_2 B}{m_3 A} - 1 \geq 1 & \gamma \geq \frac{m_3 A}{m_2 B} \\ 1 & o.w. \end{cases}$$

$$\geq 1, \tag{57}$$

where we used $m_3 A \geq m_2 B$ that can be shown by utilizing Lemma A.3. Similarly we can bound $l(\cdot)$ by

$$l(\gamma) = \frac{\gamma m_2 B - \sqrt{(\gamma m_2 B - m_3 A)^2 + (\gamma - 1) n m_2 m_3 A^2}}{m_3 A}$$

$$\leq \frac{\gamma m_2 B - |\gamma m_2 B - m_3 A|}{m_3 A} = \begin{cases} 1 & \gamma \geq \frac{m_3 A}{m_2 B} \\ \frac{2\gamma m_2 B}{m_3 A} - 1 \leq 1 & o.w. \end{cases}$$

$$\leq 1 \tag{58}$$

Finally, as the coefficient behind the p^2 term in Equation 54 is always negative, the quadratic function is concave. Therefore, the inequality holds if and only if $q\, u(\gamma) = p_1^* \geq p \geq= p_2^* = q\, l(\gamma)$.

□

Proof of Theorem 2.6. We use a similar terminology as the proof of Theorem 2.5.
First, we find P'_{ij} after closing a γ-homophilous edge:

$$P'_{ij} = \begin{cases} p' = p + (1-p)\frac{\gamma}{o_\gamma} & type(i) = type(j) \\ q' = q + (1-q)\frac{1}{o_\gamma} & type(i) \neq type(j) \end{cases}, \tag{59}$$

where $o_\gamma = o_b + \gamma o_m$, o_m and o_b are number of monochromatic and bichromatic missing edges respectively. Defining $a = \frac{EV_2}{EV_1}$, we obtain a quadratic equation

$$a^2[n_2 q'] + a[n_1 - n_2]p' - n_1 q' = 0, \tag{60}$$

which has a single valid solution when we impose $a \geq 0$:

$$a = \frac{\beta - (n_1 - n_2)p}{2n_2 q} + \frac{1}{o_\gamma} \frac{(n_1 - n_2)}{n_2}(1-p)\Big[\frac{p(1-q)}{q(1-p)} - \gamma\Big]\frac{\beta - (n_1 - n_2)p}{2q\beta} + O\Big(\frac{1}{n^3}\Big). \tag{61}$$

A comparison of Equation 61 and Equation 9 shows triadic closure has a positive relative effect if and only if

$$\frac{n}{w}p^2(p - q) > \frac{1}{o_\gamma}(1-p)\Big[\frac{p(1-q)}{q(1-p)} - \gamma\Big]. \tag{62}$$

Simplifying this constraint, we have:

$$\gamma > \Big(\frac{p}{q}\Big)\frac{w(1-q) - o_b npq(p-q)}{w(1-p) + o_m np^2(p-q)} = \frac{p}{q}c(p, q). \tag{63}$$

Without going through details, we utilize Lemma A.1, and expand $c(p, q)$:

$$c(p, q) = \frac{(n_1^3 + n_2^3)p^2 + n n_1 n_2 q(2p + q)}{(n_1^3 + n_2^3)p^2 + n n_1 n_2 [p(2q + p) + \frac{1-p}{1-q}(q^2 - p^2)]}. \tag{64}$$

Next we bound $c(p, q)$. We first show $c(p, q) \leq 1$ by comparing the nominator and the denominator of $c(p, q)$:

$$q(2p + q) \leq p(2q + p) + \frac{1-p}{1-q}(q^2 - p^2)$$

$$\iff (p^2 - q^2)\Big[\frac{1-p}{1-q} - 1\Big] \leq 0$$

$$\iff -(p - q)^2 \leq 0. \tag{65}$$

Finally, we show $\frac{p}{q}c(p,q) \geq 1$ if and only if $p > q$:

$$(n_1^3 + n_2^3)p^3 + nn_1n_2pq(2p+q) \geq (n_1^3 + n_2^3)p^2q + nn_1n_2[pq(2q+p) + \frac{1-p}{1-q}q(q^2 - p^2)]$$

$$\iff 0 \geq -(p-q)\left[(n_1^3 + n_2^3)p^2 + nn_1n_2pq + nn_1n_2q\frac{1-p}{1-q}\right]$$

$$\iff p > q. \tag{66}$$

$\square$

PROOF OF THEOREM 3.1. Let $\theta_t \in [K]$ shows the type of the node arrived at time t and $P(\theta_t = \theta) = p(\theta)$ independent of other nodes. We name the nodes based on their arrival time. For $t + 1 > t_0$, we define

$$P_{t_0}^{t+1}(\theta_{t+1}|\theta_{t_0}) = P(\text{node } t+1 \text{ is of type } \theta_{t+1} \text{ and is connected to node } t_0). \tag{67}$$

Sometimes we represent $P_{t_0}^t(\cdot|\cdot)$ as matrix $\boldsymbol{P}_{t_0}^t \in \mathbb{R}_+^{K \times K}$. Let $n_t(\theta)$ be the total number of nodes of type θ until t, and $N = N_S + N_D + N_F$ be the total number of outbound edges from each node. For $\theta_{t+1} = \theta_{t_0} = \theta$, the mean field approximation of $P_{t_0}^{t+1}(\theta|\theta)$ is

$$P_{t_0}^{t+1}(\theta|\theta) = p(\theta)\frac{N_S}{n_t(\theta)}$$
$$+ p(\theta)\alpha N_F \frac{\sum_{\tau=t_0+1}^t P_{t_0}^\tau(\theta|\theta)}{n_t(\theta)N}$$
$$+ p(\theta)(1-\alpha)\frac{N_F}{K-1}\sum_{\theta' \neq \theta}\frac{\sum_{\tau=t_0+1}^t P_{t_0}^\tau(\theta'|\theta)}{n_t(\theta')N}. \tag{68}$$

The above equation consists of three terms; in all of them $p(\theta)$ corresponds to the probability that node $t + 1$ is of type θ. The first term of Equation 68 shows the probability that node $t + 1$ finds node t_0 in the first phase: there are $n_t(\theta)$ nodes of type θ and node $t + 1$ is going to select N_S of them, so, the probability that node t_0 is one of the N_S selected nodes is $\frac{N_S}{n_t(\theta)}$. The second term of Equation 68 shows the probability that node $t + 1$ finds node t_0 through their same type friends: the expected number of edges going out from nodes of type θ and entering node t_0 is $\sum_{\tau=t_0+1}^t P_{t_0}^\tau(\theta|\theta)$. The total number edges exiting nodes of type θ is $n_t(\theta)N$. So, the probability that node $t + 1$ finds node t_0 from the same type friends in the second phase is $\alpha N_F \frac{\sum_{\tau=t_0+1}^t P_{t_0}^\tau(\theta|\theta)}{n_t(\theta)N}$. Here we neglected that some edges exiting nodes of type θ might end in nodes which are already connected to node $t + 1$ in phase 1 because in long run these edges are negligible compared to $n_t(\theta)N$. The third term of Equation equation 68 corresponds to the probability that node $t + 1$ finds node t_0 through nodes of other types. Again $\sum_{\tau=t_0+1}^t P_{t_0}^\tau(\theta'|\theta)$ is the expected number of links from nodes of type $\theta' \neq \theta$ towards node t_0 and $n_t(\theta')N$ is the total number of links exiting nodes of type θ'. So, the probability that node $t + 1$ finds node t_0 in the second phase through nodes of type θ' is $(1-\alpha)\frac{N_F}{K-1}\frac{\sum_{\tau=t_0+1}^t P_{t_0}^\tau(\theta'|\theta)}{n_t(\theta')N}$.

Similarly, the mean field approximation of $P_{t_0}^{t+1}(\theta'|\theta)$, where $\theta' \neq \theta$, is

$$
\begin{aligned}
P_{t_0}^{t+1}(\theta'|\theta) = {}& p(\theta')\frac{N_D}{n_t(\theta)} \\
& + p(\theta')\alpha N_F \frac{\sum_{\tau=t_0+1}^{t} P_{t_0}^{\tau}(\theta'|\theta)}{n_t(\theta')N} \\
& + p(\theta')(1-\alpha)\frac{N_F}{K-1}\sum_{\theta''\neq\theta'}\frac{\sum_{\tau=t_0+1}^{t} P_{t_0}^{\tau}(\theta''|\theta)}{n_t(\theta'')N}.
\end{aligned}
\tag{69}
$$

The above equation also consists of three terms; in all of them $p(\theta')$ corresponds to the probability that node $t+1$ is of type θ'. The first term shows the probability that node $t+1$ finds node t_0 in the first phase. The second and third terms are the probability that node $t+1$ finds node t_0 in the second phase through nodes of type θ' and $\theta'' \neq \theta'$, respectively.

We approximate $n_t(\theta)$ in Equations 68 and 69 with its expected value: $n_t(\theta) = p(\theta)t$. To simplify the equations and to be consistent with original definitions and proofs of the Jackson-Rogers model [9], we define new variables:

$$
m_r := \frac{N_S + N_D}{N}
$$

$$
m_s := \frac{N_F}{N}
$$

$$
[P]_{\theta',\theta} := p(\theta)1_{\theta'=\theta}
$$

$$
[P_r]_{\theta',\theta} = P_r(\theta',\theta) := \begin{cases} \frac{N_S}{N_S+N_D} & \theta' = \theta \\ \frac{1}{K-1}\frac{N_D}{N_S+N_D} & o.w. \end{cases}
$$

$$
[B_r]_{\theta',\theta} := [PP_rP^{-1}]_{\theta',\theta} = \frac{p(\theta')P_r(\theta',\theta)}{p(\theta)}
$$

$$
[P_s]_{\theta',\theta} = P_s(\theta',\theta) := \begin{cases} \alpha & \theta' = \theta \\ \frac{1}{K-1}(1-\alpha) & o.w. \end{cases}
$$

$$
[B_s]_{\theta',\theta} := [PP_sP^{-1}]_{\theta',\theta} = \frac{p(\theta')P_s(\theta',\theta)}{p(\theta)}
$$

$$
[\Pi_{t_0}^{t}]_{\theta',\theta} = \Pi_{t_0}^{t}(\theta'|\theta) := \sum_{\tau=t_0+1}^{t} P_{t_0}^{\tau}(\theta'|\theta).
\tag{70}
$$

Now we can merge Equations 68 and 69 into a single equation with matrix operations:

$$
P_{t_0}^{t+1} = \frac{Nm_r}{t}B_r + \frac{m_s}{t}B_s\Pi_{t_0}^{t}.
\tag{71}
$$

The LHS of Equation 71 can be approximated by $P_{t_0}^{t+1} = \Pi_{t_0}^{t+1} - \Pi_{t_0}^{t} \approx \frac{\partial \Pi_{t_0}^{t}}{\partial t}$. Then Equation 71 will be a differential equation for $\Pi_{t_0}^{t}$. Given the initial condition $\Pi_{t_0}^{t_0} = 0$, the solution of this equation is

$$
\Pi_{t_0}^{t} = \frac{Nm_r}{m_s}\left[(\frac{t}{t_0})^{m_sB_s} - I\right]B_s^{-1}B_r,
\tag{72}
$$

where by definition $(\frac{t}{t_0})^{m_sB_s} = \sum_{\mu=0}^{\infty}\frac{1}{\mu!}(m_s\ln(\frac{t}{t_0}))^{\mu}B_s^{\mu}$. B_s is invertible iff P_s is invertible. From Lemma A.4, P_s is also invertible iff $\alpha > \frac{1}{K}$.

The variable $\Pi_{t_0}^{t}(\theta'|\theta)$ shows the expected number of edges to node t_0 from nodes of type θ' arrived until t, given type of node t_0 is θ. So, the expected number of monochromatic edges

connected to node t_0 at time t is:

$$\text{mono}_{t_0}^t = \sum_{\theta \in [K]} p(\theta) \Pi_{t_0}^t(\theta|\theta) = \text{Tr}(\boldsymbol{P}\boldsymbol{\Pi}_{t_0}^t). \tag{73}$$

Plugging Equation 72 into Equation 73:

$$\text{mono}_{t_0}^t = \frac{Nm_r}{m_s} \sum_{\mu=1}^{\infty} \frac{1}{\mu!} (m_s \ln(\frac{t}{t_0}))^\mu \, \text{Tr}(\boldsymbol{P}\boldsymbol{B}_s^{\mu-1}\boldsymbol{B}_r). \tag{74}$$

Here $\text{Tr}(\boldsymbol{P}\boldsymbol{B}_s^{\mu-1}\boldsymbol{B}_r)$ can be simplified to $\text{Tr}(\boldsymbol{P}\boldsymbol{P}_s^{\mu-1}\boldsymbol{P}_r)$ using definitions from Equation 70. According to Lemma A.4, there are eigendecompositions for $\boldsymbol{P}_r$ and $\boldsymbol{P}_s$ as $\boldsymbol{V}\boldsymbol{D}_r\boldsymbol{V}^{-1}$ and $\boldsymbol{V}\boldsymbol{D}_s\boldsymbol{V}^{-1}$ (note that they have similar eigenvectors). Let's name $d_r = [\boldsymbol{D}_r]_{i,i} = \frac{KN_S/(N_S+N_D)-1}{K-1}$ and $d_s = [\boldsymbol{D}_s]_{i,i} = \frac{K\alpha-1}{K-1}$ for $i > 1$. With these representations and utilizing Lemma A.5 to calculate $\boldsymbol{V}^{-1}$, we can further simplify

$$
\begin{aligned}
\text{Tr}(\boldsymbol{P}\boldsymbol{P}_s^{\mu-1}\boldsymbol{P}_r) &= \text{Tr}(\boldsymbol{P}\boldsymbol{V}\boldsymbol{D}_s^{\mu-1}\boldsymbol{D}_r\boldsymbol{V}^{-1}) \\
&= \text{Tr}\left(\boldsymbol{P}\boldsymbol{V}\big(d_r d_s^{\mu-1}\boldsymbol{I} + (1-d_r d_s^{\mu-1})\boldsymbol{E}_{11}\big)\boldsymbol{V}^{-1}\right) \\
&= d_r d_s^{\mu-1}\,\text{Tr}(\boldsymbol{P}) + (1-d_r d_s^{\mu-1})\,\text{Tr}(\boldsymbol{P}\boldsymbol{V}\boldsymbol{E}_{11}\boldsymbol{V}^{-1}) \\
&= d_r d_s^{\mu-1} + (1-d_r d_s^{\mu-1})\,\text{Tr}(\boldsymbol{P}\frac{1}{K}\mathbf{1}) \\
&= \frac{1}{K} + \frac{K-1}{K}d_r d_s^{\mu-1},
\end{aligned}
\tag{75}
$$

where $\boldsymbol{E}_{11}$ is a matrix with only one non-zero element $[\boldsymbol{E}_{11}]_{1,1} = 1$. We also used the fact that $\text{Tr}(\boldsymbol{P}) = 1$. Plugging this result into Equation 74, we can find a simpler form for $\text{mono}_{t_0}^t$:

$$
\begin{aligned}
\text{mono}_{t_0}^t &= \frac{Nm_r}{m_s} \sum_{\mu=1}^{\infty} \frac{1}{\mu!} (m_s \ln(\frac{t}{t_0}))^\mu (\frac{1}{K} + \frac{K-1}{K}d_r d_s^{\mu-1}) \\
&= \frac{Nm_r}{Km_s}\Big[\sum_{\mu=0}^{\infty}(m_s \ln(\frac{t}{t_0}))^\mu - 1 + \sum_{\mu=0}^{\infty}(K-1)\frac{d_r}{d_s}(m_s d_s \ln(\frac{t}{t_0}))^\mu - 1 \Big] \\
&= \frac{Nm_r}{Km_s}\Big[(\frac{t}{t_0})^{m_s} - 1 + (K-1)\frac{d_r}{d_s}((\frac{t}{t_0})^{m_s d_s} - 1) \Big].
\end{aligned}
\tag{76}
$$

Our Variable of interest is the total number of monochromatic edges until time t: $\text{mono}^t = \sum_{t_0=1}^t \text{mono}_{t_0}^t$. To calculate this sum, we first observe that for any $0 \le c < 1$,

$$\int_1^{t+1} t_0^{-c} dt_0 < \sum_{t_0=1}^t t_0^{-c} < 1 + \int_1^t t_0^{-c} dt_0, \tag{77}$$

which gives $\sum_{t_0=1}^t t_0^{-c} = \frac{1}{1-c}t^{1-c} + O(1)$. Since $m_s < 1$ and $m_s d_s < 1$, we can use this approximation and find mono^t from Equation 76:

$$
\begin{aligned}
\text{mono}^t &= \frac{Nm_r}{Km_s}\Big[\sum_{t_0=1}^t(\frac{t}{t_0})^{m_s} - t + (K-1)\frac{d_r}{d_s}\big(\sum_{t_0=1}^t(\frac{t}{t_0})^{m_s d_s} - t\big) \Big] \\
&= \frac{Nm_r}{Km_s}\Big[\frac{t}{1-m_s} - t + O(t^{m_s}) + (K-1)\frac{d_r}{d_s}\big(\frac{t}{1-m_s d_s} - t\big) + O(t^{m_s d_s}) \Big] \\
&= t\frac{Nm_r}{K}\Big[\frac{1}{1-m_s} + \frac{(K-1)d_r}{1-m_s d_s} \Big] + O(t^{m_s}) + O(t^{m_s d_s}).
\end{aligned}
\tag{78}
$$

Finally, we can find the integration in long run ($t \to \infty$):

$$
\begin{aligned}
f_\infty &= \lim_{t \to \infty} f(t) = 1 - \lim_{t \to \infty} \frac{\text{mono}^t}{Nt} \\
&= 1 - \frac{m_r}{K} \left[\frac{1}{1 - m_s} + \frac{(K-1)d_r}{1 - m_s d_s} \right] \\
&= 1 - \frac{m_r}{K} \left[\frac{1 - m_s d_s + (K-1)d_r(1 - m_s)}{(1 - m_s)(1 - m_s d_s)} \right] \\
&= \left(\frac{K-1}{K} \right) \frac{(1 - d_r)(N_S + N_D) + (1 - d_s)N_F}{N_S + N_D + (1 - d_s)N_F} \\
&= \frac{N_D + (1 - \alpha)N_F}{N_S + N_D + \frac{K}{K-1}(1 - \alpha)N_F}.
\end{aligned}
\tag{79}
$$

with the convergence rate $O(t^{m_s - 1}) = O(t^{-\frac{N_S + N_D}{N}})$ as seen from Equation 78.

$\square$

PROOF OF THEOREM 3.2. For fixed N_S, N_D, and $\alpha < 1$:

$$
\begin{aligned}
\frac{\partial f_\infty}{\partial N_F} &= \frac{(N_S + N_D + \frac{K}{K-1}(1 - \alpha)N_F)(1 - \alpha) - (N_D + (1 - \alpha)N_F)\frac{K}{K-1}(1 - \alpha)}{(N_S + N_D + \frac{K}{K-1}(1 - \alpha)N_F)^2} \\
&= \frac{1 - \alpha}{(N_S + N_D + \frac{K}{K-1}(1 - \alpha)N_F)^2} (N_S - N_D \frac{1}{K-1}) > 0.
\end{aligned}
\tag{80}
$$

So, increasing N_F will increase the integration if and only if $N_S > \frac{N_D}{K-1}$. $\square$

PROOF OF THEOREM 3.3. To measure the relative effect, we assume the total number of edges a new node makes to be fixed and equals to $N = N_S + N_D + N_F$. Further, we assume $\frac{N_S}{N_D} = \gamma$. Homophily requires $\gamma > \frac{1}{K-1}$.

Defining $\beta = \frac{N_F}{N}$, we first simplify integration from Theorem 3.2:

$$
\begin{aligned}
f_\infty &= \frac{N_D + (1 - \alpha)N_F}{N - N_F + \frac{K}{K-1}(1 - \alpha)N_F} \\
&= \frac{\frac{1 - \beta}{1 + \gamma} + (1 - \alpha)\beta}{(1 - \beta) + \frac{K}{K-1}(1 - \alpha)\beta} \\
&= \frac{1}{\gamma + 1} \frac{1 + \beta[(1 - \alpha)(1 + \gamma) - 1]}{1 + \beta(\frac{1}{K-1} - \frac{K}{K-1}\alpha)}.
\end{aligned}
\tag{81}
$$

Then we have

$$
\begin{aligned}
\frac{\partial f_\infty}{\partial \beta} &= \frac{1}{\gamma + 1} \frac{(1 + \beta\frac{1 - K\alpha}{K-1})((1 - \alpha)(1 + \gamma) - 1) - (1 + \beta[(1 - \alpha)(1 + \gamma) - 1])(\frac{1 - K\alpha}{K-1})}{(1 + \beta\frac{1 - K\alpha}{K-1})^2} \\
&= \frac{1}{\gamma + 1} \frac{(1 - \alpha)(1 + \gamma) - 1 - \frac{1 - K\alpha}{K-1}}{(1 + \beta\frac{1 - K\alpha}{K-1})^2} \\
&= \left(\frac{1 - \alpha}{\gamma + 1} \right) \frac{\gamma - \frac{1}{K-1}}{(1 + \beta\frac{1 - K\alpha}{K-1})^2} > 0,
\end{aligned}
\tag{82}
$$

which shows $\frac{\partial f_\infty}{\partial N_F} = \frac{1}{N} \frac{\partial f_\infty}{\partial \beta}$ is positive if and only if there is homophily. $\square$

PROOF OF THEOREM 3.4. We use the same notation as the proof of Theorem 3.1.
Proof of part 1. Applying Equation 71 for the ith intervention, we have:

$$P_{t_0}^{T+i} = \frac{Nm_r}{T+i-1}B_r^{(T+i)} + \frac{m_s}{T+i-1}B_s\left(\Pi_{t_0}^T + \sum_{j=1}^{i-1}P_{t_0}^{T+j}\right). \tag{83}$$

Note that for $t \leq t_0$, $P_{t_0}^t$ and $\Pi_{t_0}^t$ are zero by definition. Equation 83 is recursive and can be expanded:

$$P_{t_0}^{T+i} = \frac{Nm_r}{T+i-1}B_r^{(T+i)}$$
$$+ \frac{m_s}{T+i-1}B_s\left[\Pi_{t_0}^T + m_sB_s\Pi_{t_0}^T\sum_{j=1}^{i-1}\frac{1}{T+j-1} + Nm_r\sum_{j=1}^{i-1}\frac{B_r^{(T+j)}}{T+j-1}\right] + O\left(\frac{1}{T^3}\right). \tag{84}$$

We use the notation $\Delta(variable)$ to show the change of a *variable* due to interventions, i.e., how a *variable* is changed as $N_S^{(T+i)}$ deviates from N_S. Rewriting Equation 84 with this notation and dropping $O(\frac{1}{T^3})$:

$$\Delta P_{t_0}^{T+i} = \frac{Nm_r}{T+i-1}\Delta B_r^{(T+i)} + \frac{Nm_rm_s}{T^2}B_s\sum_{j=1}^{i-1}\Delta B_r^{(T+j)}. \tag{85}$$

Here, we used the fact that $\Delta\Pi_{t_0}^T$ is zero as future interventions have no effect on previous connections. Now we can find the effect on $\Pi_{t_0}^{T+I}$. For $t_0 \leq T$, we have:

$$\Delta\Pi_{t_0}^{T+I} = \sum_{i=1}^{I}\Delta P_{t_0}^{T+i} = Nm_r\sum_{i=1}^{I}\frac{\Delta B_r^{(T+i)}}{T+i-1} + \frac{Nm_rm_s}{T^2}B_s\sum_{i=1}^{I}\sum_{j=1}^{i-1}\Delta B_r^{(T+j)}$$

$$= Nm_r\sum_{i=1}^{I}\frac{\Delta B_r^{(T+i)}}{T+i-1} + \frac{Nm_rm_s}{T^2}B_s\sum_{i=1}^{I-1}\Delta B_r^{(T+i)}(I-i)$$

$$= Nm_r\sum_{i=1}^{I}\Delta B_r^{(T+i)}\left[\frac{1}{T+i-1} + \frac{m_s(I-i)}{T^2}B_s\right]. \tag{86}$$

Note that similar equation can be found for $t_0 > T$ if we start the sum from $i = t_0 - T + 1$ in Equation 86. Next, we can find the change in number of monochromatic edges connected to node t_0 ($t_0 \leq T$) until $T+I$:

$$\Delta\text{mono}_{t_0}^{T+I} = \text{Tr}(P\Delta\Pi_{t_0}^{T+I})$$

$$= Nm_r\sum_{i=1}^{I}\left[\frac{1}{T+i-1}\text{Tr}(P\Delta B_r^{(T+i)}) + \frac{m_s(I-i)}{T^2}\text{Tr}(P\Delta B_r^{(T+i)}B_s)\right]$$

$$= Nm_r\sum_{i=1}^{I}\left[\frac{1}{T+i-1}\left(\frac{\Delta N_S^{(T+i)}}{N_S+N_D}\right) + \frac{m_s(I-i)}{T^2}\left(\frac{\Delta N_S^{(T+i)}}{N_S+N_D}\frac{K\alpha-1}{K-1}\right)\right]$$

$$= \sum_{i=1}^{I}\left[\frac{1}{T+i-1} + \frac{m_s(I-i)}{T^2}\frac{K\alpha-1}{K-1}\right]\Delta N_S^{(T+i)}. \tag{87}$$

To be concise, we didn't go through the calculation of $\text{Tr}(\cdot)$ here but it follows a similar technique as used in the proof of Theorem 3.1. Again, similar results can be obtained for $t_0 > T$ if we start the sum from $i = t_0 - T + 1$. Finally, we find the change in total number of monochromatic edges

until $T + I$

$$\Delta\text{mono}^{T+I} = \sum_{t_0=1}^{T+I-1} \Delta\text{mono}_{t_0}^{T+I} = \sum_{i=1}^{I} \left[1 + \frac{m_s(I-i)}{T}\frac{K\alpha-1}{K-1}\right]\Delta N_S^{(T+i)}, \tag{88}$$

which gives the change of integration at time $T + I$ as:

$$\Delta f(T+I) = -\frac{\Delta\text{mono}^{T+I}}{N(T+I)} = -\frac{1}{N(T+I)}\sum_{i=1}^{I}\left[1 + \frac{m_s(I-i)}{T}\frac{K\alpha-1}{K-1}\right]\Delta N_S^{(T+i)}. \tag{89}$$

This completes the first part of the proof.

Proof of part 2. Equation 71 explains the network dynamic after interventions. Approximating $P_{t_0}^{t+1} = \Pi_{t_0}^{t+1} - \Pi_{t_0}^{t}$ by $\frac{\partial\Pi_{t_0}^t}{\partial t}$ gives a differential equation for $\Pi_{t_0}^t$ that has the general solution:

$$\Pi_{t_0}^t = \frac{Nm_r}{m_s}(\frac{t}{c_1})^{m_s B_s} B_s^{-1} B_r C_2 \tag{90}$$

where c_1 and C_2 should be determined by initial conditions.[3] Let $c_1 = T + I$, the initial condition requires:

$$\frac{Nm_r}{m_s}B_s^{-1}B_r C_2 = \Pi_{t_0}^{T+I}. \tag{91}$$

The linear relationship of C_2 and $\Pi_{t_0}^{T+I}$ makes it easy to use our Δ notation:

$$\Delta C_2 = \frac{m_s}{Nm_r}B_r^{-1}B_s\Delta\Pi_{t_0}^{T+I}, \tag{92}$$

where $\Pi_{t_0}^{T+I}$ can be plugged in from Equation 86. We can then find the change of $\Pi_{t_0}^t$ due to interventions:

$$\Delta\Pi_{t_0}^t = (\frac{t}{T+I})^{m_s B_s}\Delta\Pi_{t_0}^{T+I}. \tag{93}$$

The change in number of monochromatic edges connected to node t_0 ($t_0 \le T$) is:

$$\begin{aligned}
\Delta\text{mono}_{t_0}^t &= \text{Tr}(P\Delta\Pi_{t_0}^t)\\
&= \sum_{\mu=0}^{\infty}\frac{1}{\mu!}(m_s\ln(\frac{t}{T+I}))^\mu \, \text{Tr}\left(PB_s^\mu\Delta B_r^{(T+i)}\Delta\Pi_{t_0}^{T+I}\right)\\
&= \frac{Nm_r}{T}\sum_{\mu=0}^{\infty}\frac{1}{\mu!}(m_s\ln(\frac{t}{T+I}))^\mu\sum_{i=1}^{I}\text{Tr}(PB_s^\mu\Delta B_r^{(T+i)}) + O(\frac{1}{T^2})\\
&= \frac{Nm_r}{T}\sum_{\mu=0}^{\infty}\frac{1}{\mu!}(m_s\ln(\frac{t}{T+I}))^\mu\sum_{i=1}^{I}\frac{K-1}{K}d_s^\mu\Delta d_r^{(T+i)} + O(\frac{1}{T^2})\\
&= \frac{Nm_r}{T}\frac{K-1}{K}\sum_{i=1}^{I}(\frac{t}{T+I})^{m_s d_s}\Delta d_r^{(T+i)} + O(\frac{1}{T^2})\\
&= \frac{1}{T}\sum_{i=1}^{I}(\frac{t}{T+I})^{m_s d_s}\Delta N_S^{(T+i)} + O(\frac{1}{T^2}).
\end{aligned} \tag{94}$$

---

[3]Note that we could embed c_1 into C_2 but the current representation makes it easier for us to apply initial conditions.

Here, we used a result from the proof of Theorem 3.1 to calculate the trace function (Equation 75). We should also note that similar results can be obtained for $t_0 > T$ by starting the sum from $i = t_0 - T + 1$. Now we can find the effect on the total number of monochromatic edges:

$$\Delta\text{mono}^t = \sum_{t_0=1}^{t} \Delta\text{mono}_{t_0}^t = \sum_{i=1}^{I} (\frac{t}{T+I})^{m_s d_s} \Delta N_S^{(T+i)} + O(\frac{1}{T}). \tag{95}$$

Finally, dropping $O(\frac{1}{T})$ from Δmono^t, the effect on integration is:

$$\Delta f(t) = -\frac{\Delta\text{mono}^t}{Nt} = -\frac{1}{N}\sum_{i=1}^{I}(\frac{t}{T})^{m_s d_s}\Delta N_S^{(T+i)} \tag{96}$$

where $d_s = \frac{K\alpha-1}{K-1}$ and $m_s = \frac{N_F}{N}$.

$\square$

PROOF OF THEOREM 4.1. Let $\Theta = \{1, 2\}$ be the set of possible types of nodes and n_θ shows the relative size of the group with type $\theta \in \Theta$. We define the following variables:

- $(T^k)_{\theta'|\theta}$: starting from a node of type θ and going to neighbor nodes, the probability of ending in a node of type θ' in k steps.
- $P_{\theta',\theta}$: the probability that a randomly selected edge is between nodes of types θ' and θ ($P_{\theta',\theta} = P_{\theta,\theta'}$ by definition).
- $M_{\theta'|\theta}$: the probability that in an iteration a new edge is formed between nodes of types θ' and θ given that the focal node is of type θ.

The mean field approximation for $M_{\theta'|\theta}$ is:

$$M_{\theta'|\theta} = (1-c)n_{\theta'}S_{\theta',\theta} + c(T^2)_{\theta'|\theta}S'_{\theta',\theta}, \tag{97}$$

where the first term corresponds to the case that the candidate node is found uniformly at random and the second term corresponds to triadic closure. Let's define one step in time equivalent to L iterations where L is the total number of links. The mean field approximation for time derivative of $P_{\theta,\theta}$ is:

$$\frac{dP_{\theta,\theta}}{dt} = n_\theta M_{\theta|\theta} - n_\theta(\sum_{\theta'\in\Theta} M_{\theta'|\theta})T_{\theta|\theta}. \tag{98}$$

Here, the first term is the probability that the focal node is of type θ and has created a link to a similar candidate node. The second term is the probability that after successfully creating a new edge, an edge between two nodes of type θ is removed. As we only have two types of nodes in our setup, we use $\bar{\theta}$ to show the other type: $\{\bar{\theta}\} = \Theta \setminus \{\theta\}$. By plugging Equation 97 into Equation 98:

$$\begin{aligned}\frac{dP_{\theta,\theta}}{dt} =& n_\theta\big[(1-c)n_\theta s + c(T^2)_{\theta|\theta}\big] \\ &- n_\theta T_{\theta|\theta}\big[(1-c)n_\theta s + c(T^2)_{\theta|\theta}s' + (1-c)n_{\bar{\theta}}(1-s) + c(T^2)_{\bar{\theta}|\theta}(1-s')\big].\end{aligned} \tag{99}$$

The (T^2) terms can be expanded recursively:

$$(T^2)_{\theta'|\theta} = \begin{cases} T_{\theta|\theta}^2 + T_{\bar{\theta}|\theta}T_{\theta|\bar{\theta}} = T_{\theta|\theta}^2 + (1-T_{\theta|\theta})(1-T_{\bar{\theta}|\bar{\theta}}) & \theta' = \theta \\ T_{\theta|\theta}T_{\bar{\theta}|\theta} + T_{\bar{\theta}|\theta}T_{\bar{\theta}|\bar{\theta}} = T_{\theta|\theta}(1-T_{\theta|\theta}) + (1-T_{\theta|\theta})T_{\bar{\theta}|\bar{\theta}} & \theta' = \bar{\theta} \end{cases}. \tag{100}$$

We used $T_{\bar{\theta}|\theta} = 1 - T_{\theta|\theta}$ in obtaining the above equation. By plugging this expansion into Equation 99, $dP_{\theta,\theta}/dt$ will be a function of $T_{\theta|\theta}$ and $T_{\bar{\theta}|\bar{\theta}}$ only.
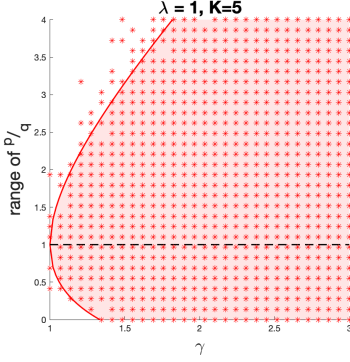
Fig. 8. $u(\gamma)$ and $l(\gamma)$ for balanced groups. The shaded area is obtained by theory. Marks show positive relative effects in simulations.
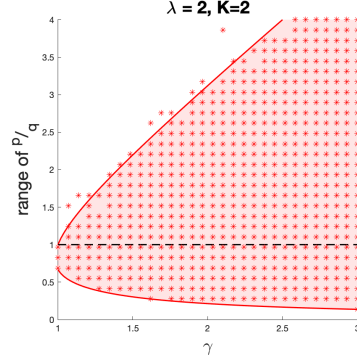
Fig. 9. $u(\gamma)$ and $l(\gamma)$ for unbalanced groups. The shaded area is obtained by theory. Marks show positive relative effects in simulations.

Although we cannot directly solve these differential equations, we can look into equilibrium that happens at the fixed points of equations. In fixed points, $dP_{\theta,\theta}/dt = 0$ for all $\theta \in \Theta$:

$$\frac{dP_{1,1}}{dt}(T_{1|1}, T_{2|2}) = 0 \tag{101}$$

$$\frac{dP_{2,2}}{dt}(T_{1|1}, T_{2|2}) = 0. \tag{102}$$

By solving these coupled equations for $T_{1|1}$ and $T_{2|2}$, we find all fixed points. Then based on the second derivatives, we keep only the stable ones (look at Asikainen et al. [5] for details on distinguishing stable fixed points).

Finally, there is a one-to-one relationship between $T_{1|1}, T_{2|2}$ and $P_{1,1}, P_{2,2}$:

$$T_{\theta|\theta} = \frac{2P_{\theta,\theta}}{2P_{\theta,\theta} + P_{\theta,\bar{\theta}}} = \frac{2P_{\theta,\theta}}{1 + P_{\theta,\theta} - P_{\bar{\theta},\bar{\theta}}}, \quad \theta \in \Theta \tag{103}$$

that can be solved to find $P_{1,1}$ and $P_{2,2}$ in terms of $T_{1|1}$ and $T_{2|2}$. The network integration is simply $1 - P_{1,1} - P_{2,2}$. Figure 3 shows network integration at stable fixed points for $n_1 = n_2 = \frac{1}{2}$ and $s' = \frac{1}{2}$, while varying s. One can see that increasing c consistently increases (decreases) integration when $s > \frac{1}{2}$ ($s < \frac{1}{2}$).

□

B SIMULATIONS

First of all, we investigate stochastic block models through simulation. Specifically, we test Theorem 2.4 as Theorems 2.1 and 2.2 can be seen as special cases of this theorem for $\gamma = 0$ and $\gamma \to \infty$, respectively. From Theorem 2.4 we expect triadic closure to have positive relative effect when $u(\gamma) > \frac{p}{q} > l(\gamma)$. To test this theorem, we have simulated a stochastic block model consisting of K groups, where group k has $n_k = 10\,\lambda^k$ members. We use various values of $\frac{p}{q}$ and λ in simulations. Figures 8 and 9 show the theoretical and simulated results together. Each mark on the figures shows specific values of $\frac{p}{q}$ and γ that triadic closure has had a positive relative effect on average. One can see despite having small networks, Theorem 2.4 well predicts the effect both for balanced and unbalanced networks.
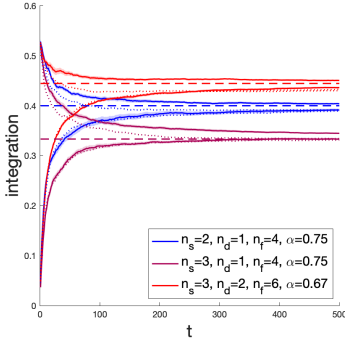
Fig. 10. Convergence of a Jackson-Rogers network. Dashed lines show predicted behavior in equilibrium by Theorem 3.1.
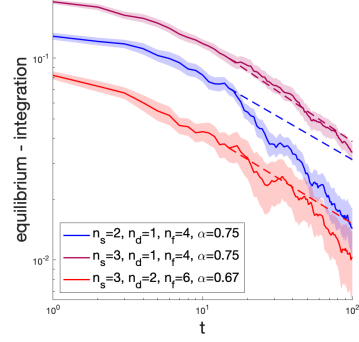
Fig. 11. The residual to reach the predicted equilibrium. Dashed lines show predicted upper bound on the convergence rate.

Next, we study the Jackson-Rogers model's convergence through simulations. Figure 10 shows network integration of a dynamic graph consisting of two groups evolving with the Jackson-Rogers model. The dashed lines show the integration in equilibrium predicted by Theorem 3.1. The solid and dotted lines show the average integration of repeated simulations for balanced and unbalanced networks. To show that behavior in equilibrium is independent of the initial network, we have run simulations for two cases: a completely segregated initial network and a fully connected initial network. It seems Theorem 3.1 can robustly predict the network's behavior for various model parameters, regardless of the initial network and distribution of groups. Further, Figure 11 shows the residual to equilibrium on a logarithmic scale. The dashed lines correspond to the convergence rate $O(t^{-\frac{N_S+N_D}{N}})$. One can see the proposed upper bound on the convergence rate also matches the behavior of the network in simulations.